AD_____

Award Number: DAMD17-98-1-8103

TITLE: Evaluation of DNA Binding Drugs as Inhibitors of ESX, an ETS Domain Transcription Factor Associated with Breast Cancer: Effects of ESX/DNA Complex Disruption

PRINCIPAL INVESTIGATOR: Stephanie J. Leslie

CONTRACTING ORGANIZATION: Health Research, Incorporated
Buffalo, New York 14263-0001

REPORT DATE: August 2001

TYPE OF REPORT: Annual Summary

PREPARED FOR: U.S. Army Medical Research and Materiel Command
Fort Detrick, Maryland 21702-5012

REPORT DOCUMENTATION PAGE

Form Approved
OMB No. 074-0188

1. AGENCY USE ONLY (Leave blank)	2. REPORT DATE	3. REPORT TYPE AND DATES COVERED
	August 2001	Annual Summary (1 Aug 00 - 31 Jul 01)

4. TITLE AND SUBTITLE
Evaluation of DNA Binding Drugs as Inhibitors of ESX, and ETS Domain Transcription Factor Associated with Breast Cancer: Effects of ESX/DNA Complex Disruption

5. FUNDING NUMBERS
DAMD17-98-1-8103

6. AUTHOR(S)
Stephanie J. Leslie

7. PERFORMING ORGANIZATION NAME(S) AND ADDRESS(ES)
Health Research, Incorporated
Buffalo, New York 14263-0001

E-Mail: Stephanie_leslie_416@mns.com

8. PERFORMING ORGANIZATION REPORT NUMBER

9. SPONSORING / MONITORING AGENCY NAME(S) AND ADDRESS(ES)
U.S. Army Medical Research and Materiel Command
Fort Detrick, Maryland 21702-5012

10. SPONSORING / MONITORING AGENCY REPORT NUMBER

11. SUPPLEMENTARY NOTES
Report contains color

12a. DISTRIBUTION / AVAILABILITY STATEMENT
Approved for Public Release; Distribution Unlimited

12b. DISTRIBUTION CODE

13. ABSTRACT ***(Maximum 200 Words)***

This work was designed to compare representative DNA-binding agents to inhibit formation of transcription factor (TF) complexes on a key gene regulatory element. This was done in an attempt to link inhibition of TF binding with decreased cellular mRNA levels. The results obtained from conventional DNA-binding agents can be used as a baseline to assess novel sequence specific ligands for improved selective inhibition of gene expression.

Most sequence preference DNA-binding agents were capable of inhibiting ESX/promoter complex formation and subsequent gene expression. However, this inhibition appeared to be non-selective since general transcription was inhibited as well. Analysis of the sequence specific polyamides, on the other hand, found limited measurable activity within a cellular environment in spite of their effective inhibition of TF binding and function in cell-free systems.

Analysis of a variety of fluorescently labeled PAs suggest that these novel ligands are cell permeable but perhaps vulnerable to cellular modification. This unidentified alteration results in a compound incapable of reaching or binding intranuclear DNA and whose fluorescence detection within the cell is precluded. The use of solvents released the quenched and bio-unavailable forms of the PAs, which then exhibited nuclear localization for most ligands. Structure-localization studies suggest that the majority (6 of 9) of PAs localize in the nucleus in a chromatin-like pattern.

14. SUBJECT TERMS
Breast Cancer

15. NUMBER OF PAGES
79

16. PRICE CODE

17. SECURITY CLASSIFICATION OF REPORT	18. SECURITY CLASSIFICATION OF THIS PAGE	19. SECURITY CLASSIFICATION OF ABSTRACT	20. LIMITATION OF ABSTRACT
Unclassified	Unclassified	Unclassified	Unlimited

Table of Contents

Annual Summary

Introduction:

Regulation of cancer associated gene expression by anti-cancer agents is our current area of research. Gene expression requires the association of transcription factors both general and gene specific to the promoter region to allow for transcription of that gene. A strategy for inhibiting gene expression is to utilize DNA binding compounds that recognize similar DNA binding motifs (based upon sequence and groove preference) as the DNA binding domain of a targeted transcription factor. It is widely assumed that agents found to be potent in reducing complex formation will be effective inhibitors of gene expression or that inhibition of gene expression in cells is a result of drug related interference with the transcription factor DNA complex. To test the validity of this scheme, drugs with differing DNA-binding motifs (minor groove or intercalating) and sequence preferences (A/T or G/C or sequence specific) were examined for correlations between their ability to inhibit formation of a targeted transcription factor/DNA complex and gene expression. The target is HER2/*neu* gene expression since it is found overexpressed in approximately 30% of all breast cancer cases. Recently an ETS family transcription factor, ESX, has been identified as a possible regulatory transcription factor of the HER2/*neu* gene. Our goal is to assess DNA-binding drugs for their ability to interfere with transcription factor (ESX) binding to the target gene's promoter region (HER2/*neu*). This work has begun to uncover drug DNA-binding motifs that can be exploited to develop new drugs or modify existing agents that could target HER2/*neu* promoter expression.

Annual Summary

Body:

Binding of basal and gene regulatory transcription factors (TFs) to a gene promoter is facilitated through a DNA binding domain which contains features responsible for sequence and topology recognition thus creating TF/DNA complexes that promote gene expression. Disruption of TF/DNA complexes by DNA binding agents that alter promoter structure are therefore expected to decrease TF function and gene expression. DNA binding agents may also be targeted to particular promoters since they of have sequence preferences (either A/T or G/C sequences) or sequence specific (synthetically designed agents called polyamides), due to available donor and acceptor groups within the DNA recognition sequence.

Using a common DNA target for assessment of how DNA binding agents can inhibit TF binding and regulated gene expression in a series of related cell-free and whole-cell studies may reveal which DNA binding motifs are the most effective for disrupting TF function. We have chosen an ETS binding sequence (EBS) on the HER2/*neu* promoter as a model system for evaluating DNA binding drugs. ETS, a large family of transcription factors, binds to the EBS, which contains a GGAA central core. A newly identified ETS transcription factor family member, ESX, is thought to contribute to the regulation of HER2/*neu* expression. The putative ESX binding sequence in the HER2/*neu* promoter, -GAGGAAGT-, lends itself to targeting by A/T and G/C sequence preference agents as well as different groove binding agents, since ETS factors like ESX contact both DNA grooves.

Understanding the mechanism of molecular regulation of a gene promoter and cell-free evaluation of how drugs can affect the individual components of this regulation are needed to develop drugs with enhanced inhibitory activity. There is a need for further development of drugs that cannot only inhibit gene expression in cells, but can do so in a manner that is based upon a DNA targeting strategy. Recent studies have found that uniquely designed sequence specific minor groove binding agents, polyamides, which are not cytotoxic, bind DNA as side-by-side dimers and are extremely effective inhibitors of TF/DNA complex formation and cell-free expression. However, there are limited examples of biological activity by polyamides. This may suggest that this family of ligands may encounter cellular barriers preventing them from reaching their designed target, nuclear DNA. Here we examined the uptake and localization of these ligands in cells. Once the cellular compartment was identified the molecular binding site of the polyamides were determined. This work has begun to uncover potential cellular barriers that impede polyamide targeting to the nucleus, perhaps due to a design flaw with the ligands.

AIM 1: Identification of DNA-binding agents that interfere with the binding of ESX to HER/2neu promoter DNA in cell-free assays:

- In accordance with Task 1 of the Statement of Work, months 1-6, assessment of DNA-binding agents for their ability to prevent ESX/HER2/*neu* complex formation was completed and summarized in the last annual report. Briefly, sequence specific polyamides were more potent inhibitors of complex formation than sequence preference DNA-binding agents. The data for the sequence preference agents is summarized in manuscript #1.

- In accordance with Task 1 of the Statement of Work, months 7-12, DNA footprinting for chosen agents were completed and summarized in the last annual report.

AIM 2: Effects of DNA-binding agents on ESX regulated expression of HER2/neu:

- In accordance with Task 2 of the Statement of Work, months 13-24, cell-free transcription assays of sequence preference and sequence specific agents was completed and summarized in the

previous annual report. Data for the sequence preference agents are summarized in the attached manuscript #1.

- In accordance with Task 2, months 25-36, this portion of the proposal was abandoned in favor of more whole-cell, biologically relevant assays for evaluation of agents as inhibitors of transcription factor binding in whole cells. This was defined in Task 3 in the previous report.

- In accordance with Task 3: part I, each DNA binding agents' ability to decrease targeted gene expression was assessed in whole-cell assays. Briefly, sequence preference agents were capable of inhibiting gene expression. However, normalization of gene expression data with cytotoxicity data demonstrated no agent capable of selectively inhibiting HER2/*neu*. This data is summarized in the attached manuscript #1. At the concentrations examined sequence specific agents were not capable of inhibiting gene expression. This apparent lack of cytotoxicity by polyamides may indicate that this new class of drugs cannot effectively enter whole cells. As described in the previous report, concern for cellular uptake led us to ask our collaborator to synthesize a fluorescently labeled polyamide (**22**).

- In accordance with Task 3: part II, cellular uptake and localization of **22** was examined in fixed cells and summarized in the previous report as well as the attached manuscript #2. Briefly, microscopic analysis of cells treated with **22** demonstrated a time dependent increase in detectable fluorescence. The appearance of the fluorescent signal in the nucleus was not the result of degradation of **2** and the subsequent release of free tag, since fluorescent tag alone only localizes to the cytoplasm. It was also found that uptake was temperature dependent since incubations at 4° resulted in no detectable uptake into the cell. Studies with the non-fluorescently labeled polyamide (**2**) suggest that the fluorescent tag does not interfere with ligands uptake or localization. This ligand, **22,** demonstrated a similar characteristic chromatin -like pattern similar to that of other known DNA-binding agents, like Hoechst 33342, Hoechst 33258 and Dapi.

  These fixed cell results suggest polyamides are capable of reaching the nucleus. However, the fact remains that at this time these agents do not exhibit cellular activity measured by northern blot analysis and cell growth inhibition. To try and understand this inconsistency we next examined the uptake and localization of these fluorescent agents in live cells. Figure 1 in Appendix A demonstrated limited punctate cytoplasmic staining following treatment with **22**. In addition to the difference in localization, the amount of detectable fluorescence in live cells was significantly less, nearly three orders of magnitude[1], than that detected in fixed cells. Since polyamides are strong DNA-binding molecules, we determined whether **22** staining in the cytoplasm co-localized with the DNA-containing mitochondria. However, cells treated with fluorescent polyamide (green) and a fluorescent mitochondrial selective stain (red) demonstrated no co-localization of fluorescent signals (Figure 2, Appendix A). Co-localization studies were then performed to ascertain if **22**'s fluorescence was co-localizing with the fluorescence from a lysosome selective stain, which might suggest organelle sequestration of polyamides by cells. Figure 3, Appendix A is a representative result of this co-localization study demonstrated co-localization in some cells while other cells demonstrated either no correspondence or no cellular uptake of **22**. These results suggest polyamides could be sequestered, degraded, modified into a fluorescently quenched and biologically inactive form or simply taken up in limited amounts. One possibility we explore is trapping of polyamides within the plasma membrane, which might result in quenching of the

[1]Detected fluorescence was measured using Image ProPlus software. The integrated optical density, or the average pixel intensity divided by image area, were measured and compared of images of live and fixed cells treated with fluorescent polyamides.

fluorescent signal. When **22**-treated cells were briefly exposed to methanol, an agent that permeabilizes the plasma membrane, images demonstrated nuclear localization with chromatin-like structures, and at a signal intensity that is more consistent with the fixed cell studies (Figure 4, Appendix A).

- In accordance with Task 4, we have assessed the molecular binding targets of polyamide **22**. To this end we performed co-localization studies with **22** and antibodies directed towards SC-35 (cellular splicing factor), and lamins A/C (nuclear envelope proteins), and propidium iodide (a known DNA-binding agent with different fluorescence properties). Result from confocal laser scanning microscopy studies demonstrated that **22** signal significantly co-localized with propidium iodide, did not co-localize with splicing factors and only minimally co-localized with envelope proteins (Figure 5, Appendix A). These results suggest **22** does bind to nuclear DNA.

- In accordance with Task 5, cellular uptake and localization were examined for a fluorescent polyamide structurally different from **22**. This was performed because differences in cellular uptake and localization have been observed between DNA-binding agents that are nearly identical in structure like Hoechst 33342 and 33258. To this end, **33** was created (Figure 6 in Appendix A). Similar to **22**, examination of **33** in fixed cells also demonstrated a time-dependent uptake of the ligand that could be inhibited by low temperatures (data not shown). However, in contrast to **22**, which bound in the nucleus in a chromatin-like manner, **33** appeared to bind to inner nuclear membrane (Appendix A, Figure 7). Since **33** demonstrated a different nuclear binding pattern in fixed cells we tried to determine its molecular binding target. To this end we employed the same techniques used to assess **22**'s potential binding site, which include antibodies towards SC-35, and lamins A/C, and propidium iodide. Results from confocal laser scanning microscopy studies demonstrated significant co-localization of **33** with nuclear envelope proteins, no co-localization with splicing factors and minimal co-localization with propidium iodide (Figure 8, Appendix A). These results suggest a different molecular binding site of structurally different polyamides. These differences caused concern since polyamides structures differ based upon DNA targeting strategy.

  Since **22** and **33** contain multiple structural differences, it was difficult to ascertain which structural change(s) resulted in this apparent change in localization. To this end, our collaborators designed seven additional fluorescently labeled polyamides, named Dyes, with rational structural changes (Figure 9, Appendix A). Similar to **22**, **33** and Dyes 1-7 also demonstrated cytoplasmic staining in live cells (data not shown). This result might suggest that polyamides as a class of agents may not be capable of reaching their designed target. The Dyes were next examined in fixed cells. No signal was detected for Dyes 1 and 2 in fixed cells. For Dyes 3-7 however, uptake was time-dependent and demonstrated a similar binding pattern to **22** (Appendix A, Figure 10). These results suggest that most polyamides bind to nuclear DNA if they can be released from their site of sequestration.

- **Key Research Accomplishments:**
  - Task 1, months 6-12: ***COMPLETE***
    - **Results**:
      - The sequence specific polyamides are by far the most potent inhibitors of complex formation.
      - When comparing different modes of binding among the sequence preference DNA binding agents it appears that the agent who caused significant helical distortion, via intercalation, was among the most potent inhibitors of ESX/HER2/*neu* complex formation.

  - Task 2, months 13-24: ***COMPLETE***
    - **Results**:
      - The sequence specific polyamides were equally as effective as the sequence preference agents in this assay.

  - Task 3, months 6-36: ***COMPLETE***
    - **Results**:
      - The sequence specific polyamides showed **no** effect on cell growth or gene expression in contrast to sequence preference agents which inhibited gene expression but did so in a non-specific manner.
      - Polyamide **22** is taken up into the nucleus of cells while avoiding the nucleoli. Polyamide **22** accumulates in the nucleus of cells over time.
      - Low temperatures (4°C) slow the cellular uptake of polyamide **22**.
      - Polyamide **22** in the presence of 10-fold excess polyamide **2** can effectively compete for uptake into the nucleus of cells.
      - Pre-treatment of cells with polyamide **22**, followed by treatment of excess polyamide **2**, shows competition for the same binding site.

  - Task 4, months 24-36: ***COMPLETE***
    - **Results**:
      - Co-localization studies with Lamins A, C: demonstrated minimal co-localization with **22**.
      - Co-localization studies with SC-35 demonstrated no co-localization with **22**.
      - Co-localization studies with propidium iodide demonstrated significant co-localization with **22**.

  - Task 5, months 24-36: ***COMPLETE***
    - **Results**:
      - **33** localized in the cytoplasm of live cells, similar to **22**.
      - **33** localized to the nucleus but in a different pattern from **22**.
      - Co-localization studies with Lamins A, C: demonstrated significant co-localization with **33**.
      - Co-localization studies with SC-35 demonstrated no co-localization with **33**.
      - Co-localization studies with propidium iodide demonstrated minimal co-localization with **33**.
      - Dyes 1-7, rationally designed and structurally different polyamides, demonstrated similar uptake and localization patterns in live cells as **22** and **33**.
      - Dyes 1 and 2 were not detectable in fixed cells.
      - Dyes 3-7 demonstrated a chromatin-like pattern, similar to **22**.

Reportable Outcomes:

- Manuscripts
  - #1: Covering the sequence preference agents was submitted to Cancer Research (08/01) entitled "Assessing the relationship between DNA-binding agents as inhibitors of Ets-HER2/*neu* promoter complexes and HER2/*neu* transcriptional expression".
  - #2. This manuscript, which covers the cellular uptake and distribution of polyamides, were completed and submitted in the previous annual report. Since our collaborator, Dr. Peter Dervan refused to sign off on any manuscripts containing data regarding polyamides at the time of their findings; other laboratories with assistance from other synthetic chemists have since found and published similar findings (1, 2). Therefore, at this time it is not likely that this data will be published.

Conclusions:

Despite understanding the mechanisms by which transcription factors (TFs) regulate gene expression at the molecular level, utilization of this information to design inhibitors has lagged. This study assessed the strategy of inhibiting gene expression by targeting DNA-binding agents to a TF binding site on a gene promoter in order to disrupt complex formation. Drugs used as gene expression inhibitors are often based upon their inhibitory activity in EMSA assays, which utilizes a purified TF and a small oligonucleotide containing just the TF consensus-binding site. However, results from EMSA studies may not be predictive of drug performance as an inhibitor of expression where regulation involves the interaction of numerous factors within a relatively large gene promoter region. This study not only analyzed drugs for their ability to inhibit the Ets TF, ESX, from binding to its consensus DNA site but also examined whether this ability corresponded to subsequent effects on cell-free and cellular expression of an Ets-regulated gene (HER2/*neu*). This study revealed the difficulty in extrapolating a drug's ability to inhibit cell-free TF/DNA complex formation to its effectiveness as an inhibitor of both cell-free and cellular gene expression. While each of these assays provide consistent evidence of drug inhibition of TF binding they cannot take into account factors in a whole cell environment that may impinge upon drug activity. Extrapolation of the cellular mRNA inhibition to equally cytotoxic drug levels revealed no agent capable of selectively inhibiting targeted gene expression. Likewise, attempts at correlating TF/DNA complex formation with cellular gene expression and cytotoxicity is difficult since we cannot ascertain if cell death was due to HER2/*neu* inhibition or to some other drug associated event. Drug effects on expression in cells may or may not be strictly related to the ability of the drug to target a particular gene promoter. Understanding the mechanism of molecular regulation of a gene promoter and cell-free evaluation of how drugs can affect the individual components of this regulation are needed to develop drugs with enhanced inhibitory activity. There is a need for further development of drugs that cannot only inhibit gene expression in cells, but can do so in a manner that is based upon a DNA targeting strategy.

Overall, this study pointed out the need for caution when extrapolating cell-free evaluations of drugs as inhibitors of TF/DNA complexes to effectiveness as inhibitors of gene expression. As new generations of more specific DNA-binding agents are developed, the use of a linked series of bioassays can help provide validation of the targeting concept. We did this for the sequence specific polyamides and found a lack of correlation between the ability to target TF binding in cell-free assays and inhibition of gene expression in whole cells suggesting that these ligands are incapable of reaching and affecting their target. Live cell studies, which showed minimal cytoplasmic staining, support the theory that these agents are not capable of reaching their nuclear target. Other laboratories have now found data to support these results. Furthermore, our studies with cell permeabilizing agents suggest these agents are possibly trapped or modified, which subsequently impedes fluorescent detection within live cells. Once released

from their site of sequestration/modification most ligands (6 of 9) are appear to bind intranuclear chromatin.

Lastly, this study suggests that polyamides as a class of agents have some unidentified design flaw(s) that might render them vulnerable to cellular inactivation or sequestration, which prevents nuclear targeting. A systematic study needs to be undertaken to develop these ligands into biologically active compounds. While years have been spent in the development PAs as high affinity DNA-binding ligands the idea should be kept in mind that some sacrifice in DNA binding affinity may be required to obtain a biologically activity ligand. Lastly, we need to ask, "What makes a polyamide a polyamide?" For instance, what properties are required? Is it the high binding affinity, the hairpin structure, or that fact that they can target particular sequences? When do these ligands cross over from sequence preference agents to sequence specific ligands? There are many pharmacological questions that need to be asked and answered. The results presented in this work are the first to point to the need for pharmacological analyses of these ligands as well as the necessity for redesigning polyamides into biologically active agents.

References:

1. Janssen, S., T. Durussel, and U. Laemmli. Chromatin opening of DNA satellites by targeted sequence-specific drugs. *Molecular Cell* **6**(5):999-1011 (2000).
2. Sharma, S., A. morrissey, G. Miller, W. Gmeiner, and J. Lown. Design, synthesis and intracellular localization of a florescently labeled DNA binding polyamide related to the antibiotic distamycin. *Bioorganic & Medicinal Chemistry Letters* **11**(6):769-772 (2001).

See additional references sited in the attached manuscripts.

Appendices:

A. Figures for Tasks 3-5.

B. Manuscript submitted to Cancer Research (08/01):
"Assessing the relationship between DNA-binding agents as inhibitors of Ets-HER2/*neu* promoter complexes and HER2/*neu* transcriptional expression."

C. Manuscript draft that will not be submitted for publication:
"Polyamide 2, a sequence specific DNA-binding ligand is sequestered in the cell nucleus following uptake in SKBR3 human breast cancer cells."

Appendix A

Figures for Task 3-5

Figure 1: Determination of the subcellular localization of fluorescently labeled polyamide 22 in live cells. SK-Br-3 cells were grown on cover slips and treated with **22** at 0.5 μM for 4 hour in the presence of chloroquine (CL, 100μM). Cells were then washed in room temperature PBS, removed and placed cell side down on a slide and visualized by epifluorescence microscopy. The top panel contains a bright field image while the lower panel is corresponding fluorescent image. *Imaging system,* SPOT RT. *Camera exposure*, 500 msec. *Scale bar*, 20 μm.

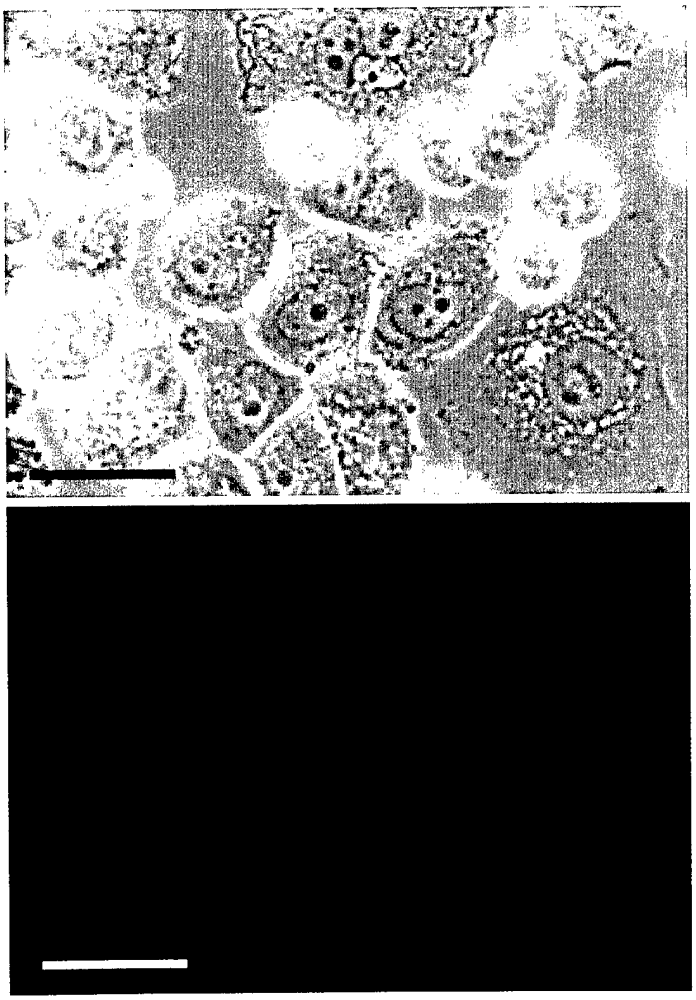

Figure 2: Comparison of the localization of 22's fluorescence with LysoTracker fluorescence. SK-Br-3 cells were grown on cover slips and treated with a simultaneous 4-hour exposure of CL (100 μM) and **22** (0.5 μM) followed by a 1-hour incubation with LysoTracker (25 nM). Cells were then washed in room temperature PBS, removed and placed cell side down on a slide and visualized by epifluorescence microscopy. The upper panel shows the localization of the lysosome-selective stain, LysoTracker. The middle panel shows the localization of **22** fluorescence. The bottom panel shows cells with co-localization (yellow arrows), cells with both stains but no co-localization (white arrows) and cells without **22** fluorescence (blue arrows). *Imaging system,* SPOT RT. *Camera exposure*, 2 sec. *Scale bar*, 20 μm.

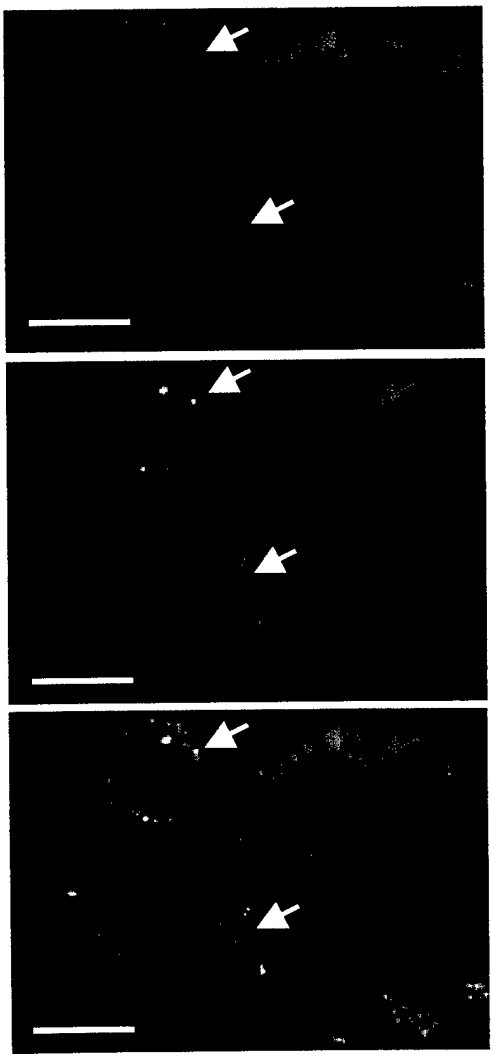

Figure 3: Comparison of the localization of 22's fluorescence with MitoTracker fluorescence. SK-Br-3 cells were grown on cover slips and treated with a simultaneous 4-hour exposure of CL (100 μM) and **22** (0.5 μM) followed by a 1-hour incubation with MitoTracker (10 nM). Cells were then washed in room temperature PBS, removed and placed cell side down on a slide and visualized by epifluorescence microscopy. The top panel shows the localization of the mitochondria-selective stain, MitoTracker. The middle panel shows the localization of **22** fluorescence. The bottom panel demonstrates no co-localization of the fluorescence signals. *Camera exposure*, 500 msec for ***upper panel*** and 2 sec for ***middle panel***. *Imaging system,* SPOT RT. *Scale bar*, 20 μm.

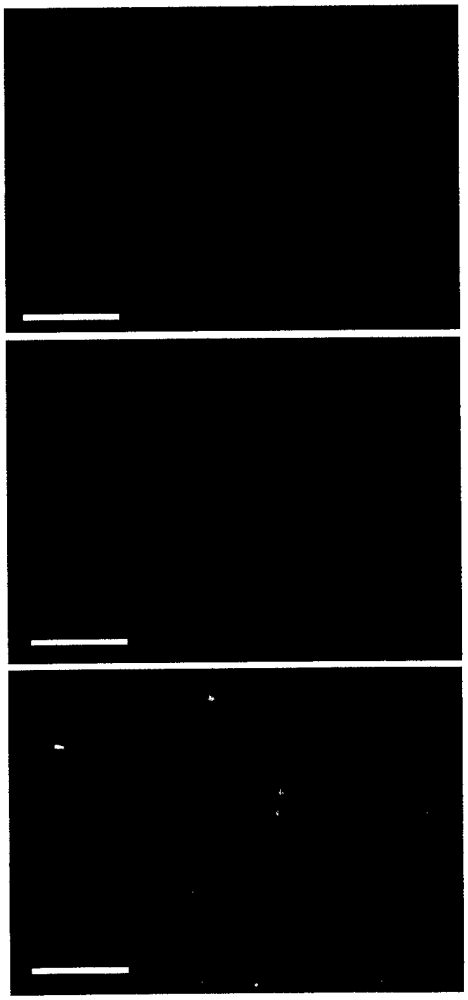

Figure 4: Effects of methanol wicking on 22's fluorescence signal and localization. SK-Br-3 cells were exposed to **22** (0.5 μM) for 4-hours. Bright field images (top panels) and fluorescence images (middle panel) were captured prior to the methanol wicking. A fluorescent image was then captured after wicking. Imaging system, SPOT RT. Exposure time, 2 sec prior to methanol wicking, and 500 msec post methanol wicking. Scale bar, 50 μm.

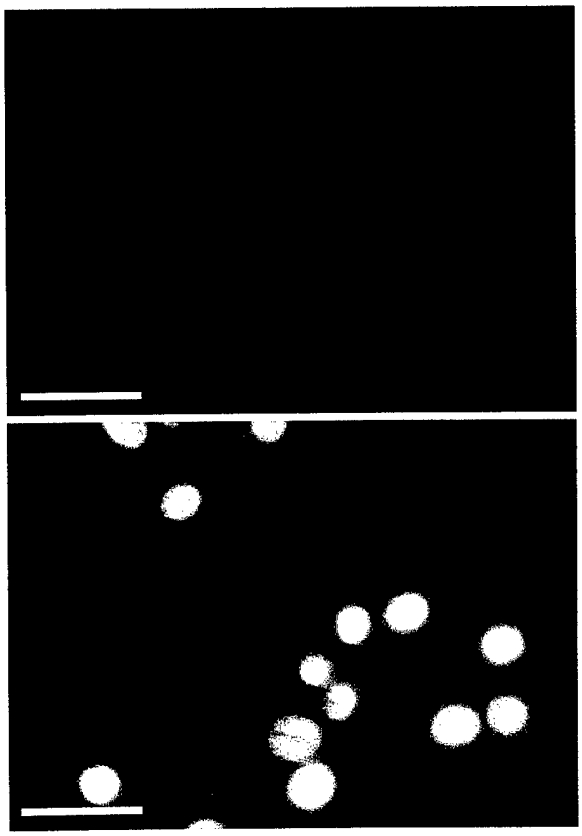

Figure 5: Laser scanning confocal microscopic analysis of 22's molecular binding site. SK-Br-3 cells were exposed to **22** (0.5 μM) for 1-hour. The cells were then fixed and probed with indicated antibody. The only exception was co-localization with propidium iodide that involved a simultaneous exposure to **22** (0.5 μM) and propidium iodide (100 μM) for 1 hour followed by fixation. The left panel is **22** and SC-35. The middle panel is **22** and lamins A/C. The right panel is **22** and propidium iodide. Regions of co-localization appear yellow. All images are 0.5 micron midplane sections. *Fixative*, methanol. *Imaging system*, BioRad MRC-1024. *Scale bar*, 20 μm.

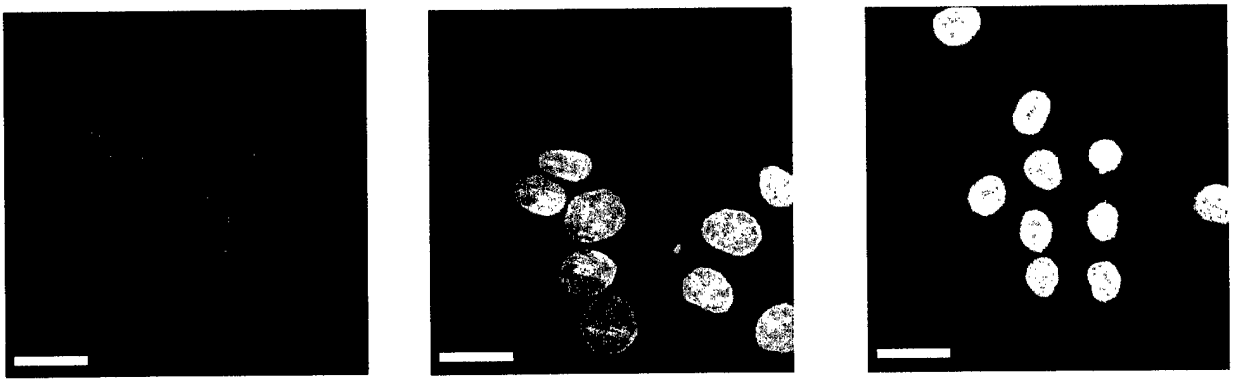

Figure 6. Two structurally different fluorescently labeled polyamides. **3** was chosen to be fluorescently labeled since it binds to the same promoter binding site as **2** but contains two β-alanine spacers in place of two pyrrole rings

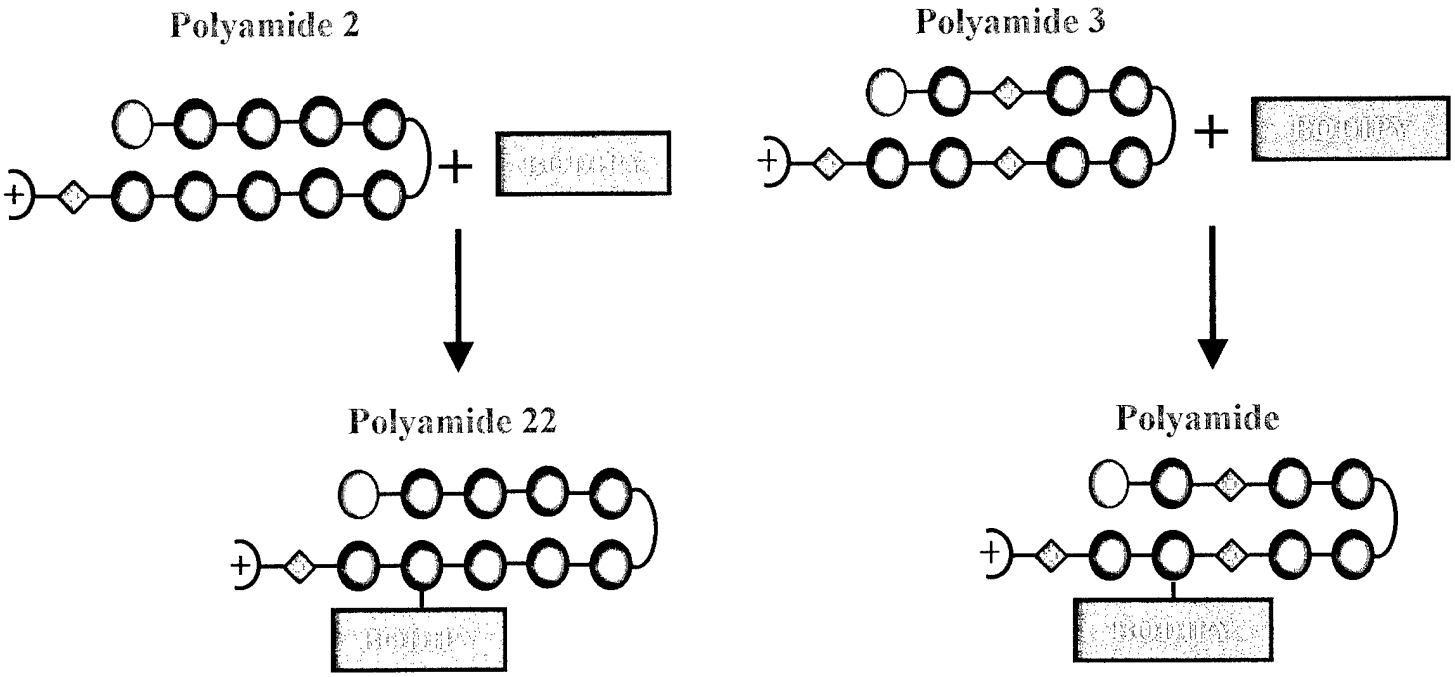

Figure 7: Comparison of cellular localization and binding pattern of 33 with 22 in fixed cells by epifluorescence microscopy. SK-Br-3 cells were treated for 1 hour with 0.5 μM: The left panel is **33** while the right panel is **22**. *Fixative*, methanol. *Imaging system*, SPOT RT. *Camera exposure*, 500 msec. *Scale bar*, 20 μm.

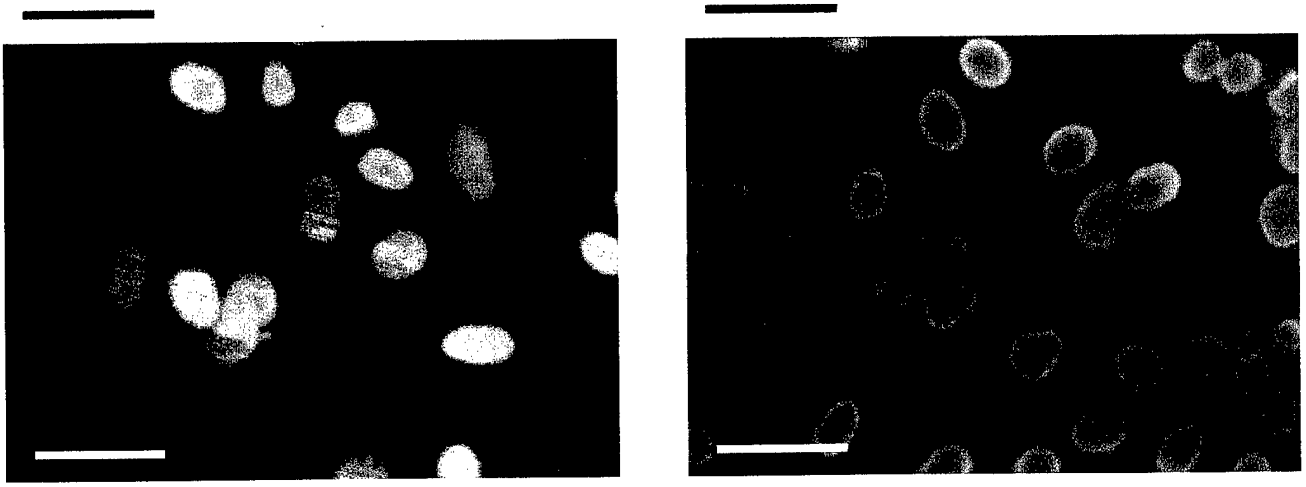

Figure 8: Laser scanning confocal microscopic analysis of 22's molecular binding site. SK-Br-3 cells were exposed to **33** (0.5 μM) for 1-hour. The cells were then fixed and probed with indicated antibody. The only exception was co-localization with propidium iodide that involved a simultaneous exposure to **33** (0.5 μM) and propidium iodide (100 μM) for 1 hour followed by fixation. The left panel is **33** and SC-35. The middle panel is **33** and lamins A/C. The right panel is **33** and propidium iodide. Regions of co-localization appear yellow. All images are 0.5 micron midplane sections. *Fixative*, methanol. *Imaging system*, BioRad MRC-1024. *Scale bar*, 20 μm.

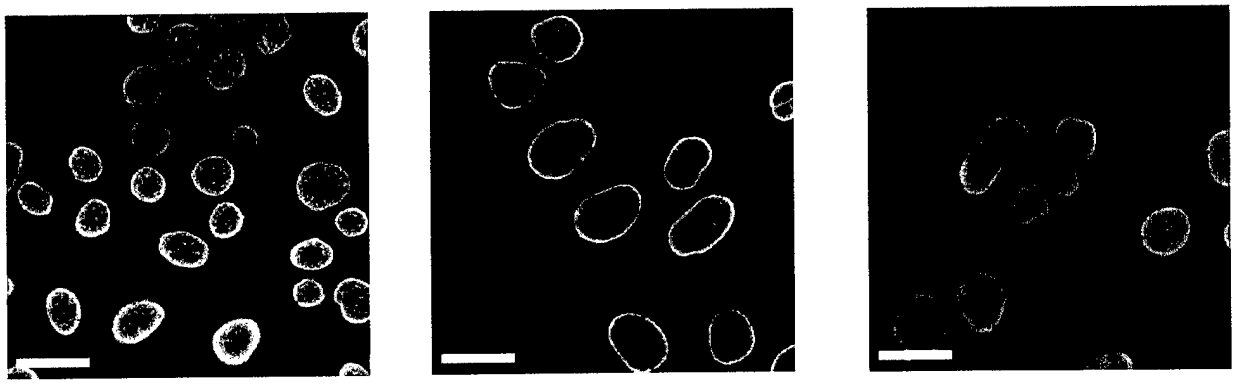

Figure 9: Structures of rationally designed Dyes. Dye 1 is the potential cleavage product of **33**. Dye 2 is a polyamide similar in ring number and composition as distamycin. Dye 3 is a combination of top arm of **33** and the bottom arm of **22**. Dye 4 and Dye 5 have the same ring number but different ring composition. Dye 6 has multiple structural changes compared with **22** and Dye 3. Dye 7 has the same polyamide backbone as **22** but contains Tamra fluorescent tag rather than Bodipy.

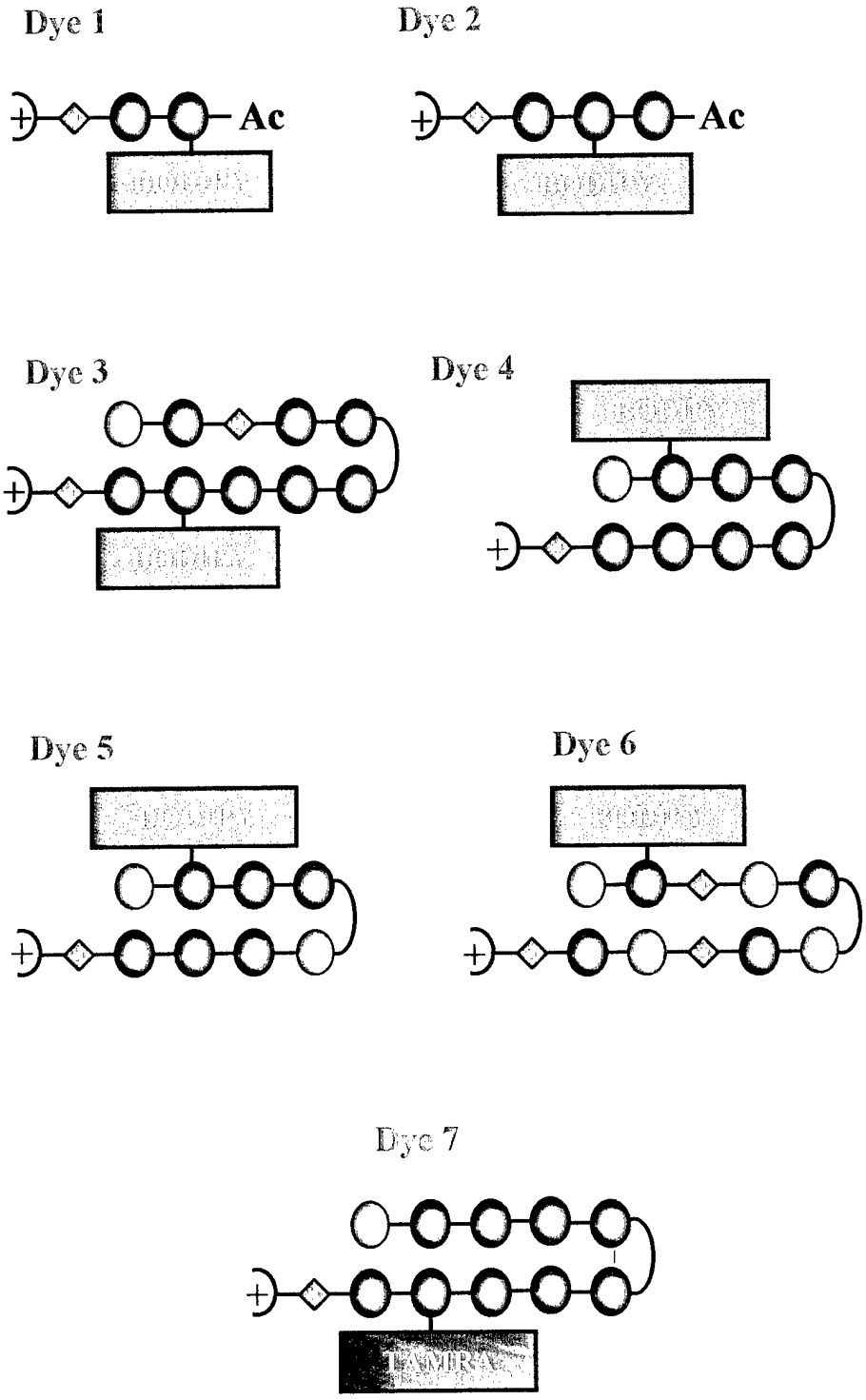

Figure 10: Dye localization in fixed cells. SK-Br-3 cells grown on cover slips were treated for 1 hour with each Dye at 0.5 μM. Cells were washed twice in PBS, and fixed in methanol prior to viewing by epifluorescence microscopy. The left side contains the bright field images while the right side is the corresponding fluorescence image with the Dye indicated on the images. *Imaging system*, SPOT RT. *Camera exposure: Dye 1 and 2, 2 sec; Dye 3, 4 and 5, 500 msec; Dye 6, 7 and 22, 100 msec.*

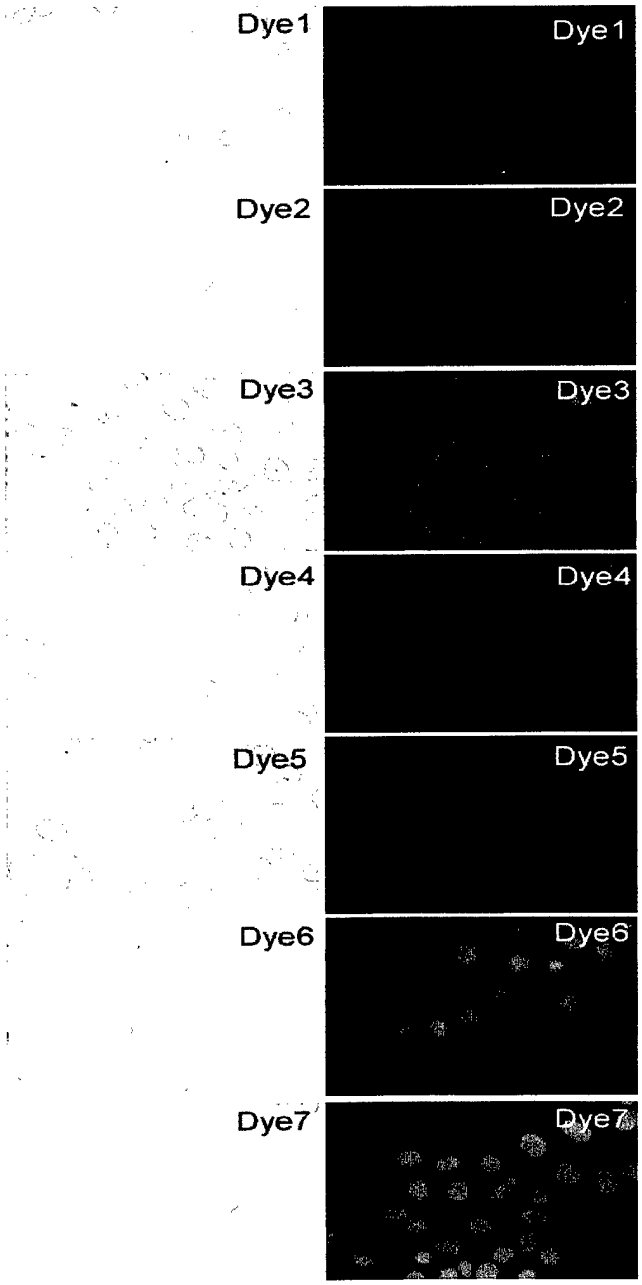

Appendix B

Manuscript #1

"Assessing the relationship between DNA-binding agents as inhibitors of Ets-HER2/*neu* promoter complexes and HER2/*neu* transcriptional expression."

Title: Assessing the relationship between DNA-binding agents as inhibitors of Ets-HER2/*neu* promoter complexes and HER2/*neu* transcriptional expression[1].

Authors: Stephanie J. Leslie, Gary K. Scott, Chris C. Benz, and Terry A. Beerman[2]

Department of Molecular Pharmacology and Experimental Therapeutics, Roswell Park Cancer Institute, Buffalo, NY 14263 [S.J.L., T.A.B.]; Department of Cancer and Developmental Therapeutics, Buck Institute for Age Research, Novata, CA 94945 [G.K.S., C.C.B.]

Running Title: Activity of DNA-binding drugs in comparative bioassays.

Key Words: DNA-binding drugs HER2/*neu* promoter-targeted Transcript-inhibiting Growth inhibition Correlation

Footnotes:

[1]This study was supported in part by grants from US Army Medical Research Grants BC980067 (to TAB), DAMD17-98-1-8103 (to SJL), American Cancer Society RPG-96-034-04-CDD (to TAB), NIH CA 36773 and NIH CA58207 (to CCB).

[2]To whom correspondence and reprint requests should be addressed: Terry Beerman, Department of Pharmacology and Therapeutics, Roswell Park Cancer Institute, Elm and Carlton Streets, Buffalo, New York 14263. Tel: 716-845-3443; Fax: 716-845-8857; e-mail: terry.beerman@roswellpark.org

[3]The abbreviations used are: TF, transcription factor; EMSA, electrophoretic mobility shift assay; MGB, minor groove binder; EBS, Ets binding site; IC_{50}, 50% inhibition concentration; GAPDH, glyceraldehyde 3-phosphate dehydrogenase; IC, internal control; SD, standard deviation.

Abstract:

A strategy for inhibiting gene expression is to utilize DNA binding compounds that recognize similar DNA binding motifs (based upon sequence and groove preference) as the DNA binding domain of a targeted transcription factor. It is widely assumed that agents found to be potent in reducing complex formation will be effective inhibitors of gene expression or that inhibition of gene expression in cells is a result of drug related interference with the transcription factor DNA complex. To test the validity of this scheme, drugs with differing DNA-binding motifs (minor groove or intercalating) and sequence preferences (A/T or G/C) were examined for correlations between their ability to inhibit formation of a targeted transcription factor/DNA complex and gene expression. Drug effects on HER2/*neu* promoter binding by ESX, a member of the Ets family of transcription factors, and disruption of the ESX/HER2/*neu* complex were analyzed using a cell-free electrophoretic mobility shift assay. Hoechst 33342, distamycin and hedamycin effectively prevented ESX binding to the HER2/*neu* promoter while chromomycin A_3 was considerably less active. In contrast, in cell-free transcription experiments, chromomycin A_3 was among the most potent inhibitors of HER2/*neu* expression, followed by distamycin and Hoechst 33342, while hedamycin was the least effective. Drug treatment of SK-Br-3 cells, a human breast adenocarcinoma cell line which overexpresses both HER2/*neu* and ESX, revealed hedamycin and chromomycin A_3 to be highly potent inhibitors of HER2/*neu* mRNA transcription while Hoechst 33342 and distamycin were relatively weak inhibitors. Ultimately, the most potent inhibitors of cellular mRNA transcription were the most cytotoxic suggesting that effects on expression were not necessarily directly related to the drug's ability to target the transcription factor/DNA complex. This study points out the need for caution when extrapolating cell-free evaluations of drugs as inhibitors of transcription factor/DNA complexes to effectiveness as inhibitors of gene expression. Additionally, these results revealed that no agent was capable of

selectively inhibiting targeted gene expression. As new generations of more specific DNA binding agents are developed, the use of a linked series of bioassays can help provide validation of the targeting concept.

Introduction:

Agents, which bind preferentially to A/T and G/C sequences, can be targeted to particular gene promoters containing the DNA recognition sequence [1-5]. For example, the crescent-shaped DNA minor groove binder (MGB), distamycin, binds preferentially to A/T sequences causing the minor groove to widen and the major groove to narrow [6-9]. This agent was found to effectively block formation of TATA box binding protein/DNA complexes [10-13]. Similarly, chromomycin A_3, which binds G/C rich regions of DNA within the minor groove, can disrupt TF/DNA complexes due to the significant distortion of the helix that occurs upon its binding [2, 14-17]. Chromomycin A_3's effective inhibition of binding by early growth response gene-1 (a G/C-preference major groove binding protein) as well as TATA box binding protein (an A/T-preference minor groove binding protein) are linked to its ability to induce helical alterations that can affect protein binding to either groove [13]. Intercalators are another class of DNA-binding agents, which alter DNA conformation by sliding their chromophore between the base pairs of DNA and lengthening the helix [4, 9, 18-21]. By altering the positions of donor/acceptor groups that participate in transcription factor (TF) site recognition, intercalators such as hedamycin have been shown to effectively disrupt a variety of TF/DNA complexes including early growth response gene-1, Wilms tumor suppressor gene-1 and TATA box binding protein [12, 13, 22].

While it is apparent that TF DNA-binding domains can be targeted by DNA-binding drugs, whether the disruption of the TF promoter complex, inhibition of gene expression, and cellular response are linked is less clear. In fact, differing results have been observed when drug-induced inhibition of TF binding to promoter response elements and inhibition of gene expression in both cell-free and whole cell assays is compared [22-25]. Also, a recent study suggested that for some DNA-binding drugs a decrease in cellular gene expression is more likely associated with general cytotoxicity than with targeted gene inhibition [26].

The present study compared agents with differing DNA-binding specificities to inhibit formation of TF complexes on a key gene regulatory element. Drug affects in cell-free assays (EMSA and *in vitro* transcription) are compared to RNA expression and growth inhibition of a cultured human breast cancer cell line (SK-Br-3). The viability and proliferation of SK-Br-3 cells depends on overexpression of the HER2/*neu* (ErbB2) oncogene, which requires an intact Ets binding site (EBS) [27-34]. This EBS (GAGGAAGT) can be targeted by either A/T or G/C sequence specific agents. The four DNA-binding antibiotics examined in this study include the A/T sequence preferring minor groove binding agents distamycin and Hoechst 33342, the G/C sequence preferring minor groove-binding agent chromomycin A_3, and the G/C sequence preferring intercalator hedamycin. Whether the potency of sequence specific DNA-reactive agents as inhibitors of transcription factor/DNA complexes in cell-free assays is predictive of their ability to modulate TF function in both cell-free and cellular environments was determined.

Materials & Methods:

Drugs:

Hedamycin (5 mM), supplied by the National Cancer Institute, was prepared by dissolving in 1/10 volume 0.1 N HCl, adding 8/10 volume ddH_2O, and neutralizing with 1/10 volume 0.1 N sodium hydroxide. Stocks of distamycin (5 mM; Sigma, St. Louis, MO) and Hoechst 33342 (20 mM; Aldrich, Chemical Co., Milwaukee, WI) were prepared in ddH_2O. Chromomycin A_3 (5 mM; Sigma, St. Louis, MO) was prepared in dimethylsulfoxide. All drug stocks were stored at –20°C and diluted into water immediately before use.

Cell Culture:

HER2/*neu*-amplified and -overexpressing SK-Br-3 cells (human breast adenocarcinoma) were purchased from American Tissue Culture Collection (Rockville, MD) and grown in McCoy's 5a medium (GIBCO, Grand Island, NY) with 10% fetal bovine serum. Cells were sub-cultured after reaching ~80% confluence ($1x10^7$ cells/T75 dish) by resuspending in medium and plating at $3x10^5$ cells/ml.

Electrophoretic Mobility Shift Assay (EMSA):

A bacterially expressed Ets protein, ESX, known to bind to the HER2/*neu* promoter's EBS, was prepared as previously described [31, 35]. Briefly, a full-length ESX cDNA was cloned into a pRSET Histidine-tag expression plasmid (NheI-HindIII; Invitrogen) and expressed in isopropylthio-β-D-galatoside induced BL21[DE3] pLysS bacteria (Stratagene, La Jolla, CA). Histidine-tagged ESX protein was purified from the bacteria by Nickel-chelate affinity chromatography, as recommended by the manufacturer (Qiagen Inc., Valencia, CA). A 34-mer

oligonucleotide (TA5-34 oligo), 5'-GGAGGAGGAGGGCTGCTT GAGGAAGTATAAGAAT-3', containing the EBS (underlined sequence), derived from the HER2/*neu* gene promoter and its complementary strand were synthesized by the Biopolymer facility (Roswell Park Cancer Institute, Buffalo, NY). The oligonucleotide was purified, annealed and end-labeled with [γ-^{32}P]-ATP using T4-polynucleotide kinase (New England BioLabs, Beverly, MA), as described previously [12, 35]. For optimization of EMSA conditions, full-length ESX protein was titrated in the presence of ^{32}P-end labeled TA5-34 oligonucleotide (1 nM) in binding buffer (30 mM potassium chloride, 5% glycerol, 25 mM Tris (pH 7.5), 0.1% NP-40, 0.1 mg/ml bovine serum albumin and 1 mM dithiothreitol). Maximal ESX/DNA complex formation (~90%) was achieved at 40 nanograms of ESX protein. A 30-minute incubation at room temperature was sufficient time to achieve equilibrium between ESX and the oligonucleotide [35]. Following complex formation, samples were electrophoresed for 60 minutes at 200 volts on a 4% polyacrylamide gel using 0.5X TBE buffer (44.5 mM Tris base, 44.5 mM boric acid, 1.0 mM ethylenediamine tetraacetic acid [pH 8.0]). Gels were dried and exposed to Kodak Biomax Scientific Imaging film. A Molecular Dynamics densitometer (Molecular Dynamics, Sunnyvale, CA) was used for quantitation of EMSA TF/DNA complexes on film and images were analyzed using ImageQuant software. The drugs' ability to disrupt the ESX/DNA complex formation was assessed by 30-minute pre-incubation of the oligonucleotide with drug, prior to the 30-minute incubation of the probe with the recombinant ESX protein and EMSA. Percent inhibition of complex formation by drug was determined by comparing the signal intensity of complex in drug-treated samples to that generated by 4 untreated controls, and IC_{50} values (amount of drug needed to inhibit 50% of complex formation) for all agents were determined.

Cell-free transcription assay:

Cesium chloride-purified plasmid DNA (RO6), containing a ~500 bp insert DNA fragment from the HER2/*neu* promoter fragment in the reporter gene expression construct pCDNA3-Luc (Invitrogen, Carlsbad, CA), was linearized with restriction enzyme, *SphI* (New England BioLabs, Beverly, MA) [36]. Nuclear extract was prepared as described previously from SK-Br-3 cells, which overexpress both HER2/*neu* and various Ets factors including ESX [35].

Radiolabeled transcripts were generated by incubation of DNA template and SK-Br-3 nuclear extract for 60 minutes in labeling cocktail containing [α-^{32}P]-CTP (800Ci/mmole; NEN, Boston, MA). Samples were extracted and electrophoresed under conditions described by Chiang et al. [35]. A PhosphorImager screen was used to visualize the ^{32}P signal from dried gels and the signal was quantified using a Molecular Dynamics PhosphorImager. T3 transcript (250 bases; Promega Co., Madison, WI) was used as an internal loading control for each sample. An RNA ladder (Gibco BRL, Grand Island, NY) of 1.77 – 0.155 kilobase pairs was dephosphorylated, end-labeled and purified as described previously and was used to verify the band of interest based on an expected HER2/*neu* transcript size of ~760 base pairs [35]. Nuclear extract was titrated in the presence of a constant amount of plasmid DNA (1 μg) to obtain the optimal signal for the 760 base pair HER2/*neu* transcript.

Inhibition of Ets-regulated gene expression was assessed by incubation of the drug with the DNA template in reaction buffer for 30 minutes at 30°C prior to addition of labeling cocktail with the Ets-containing, including ESX, SK-Br-3 nuclear extract. ImageQuant signal intensity of the HER2/*neu* reporter gene transcript (luc) for control and drug treated samples were normalized to the internal loading control signal. For each agent the percent inhibition of transcript formation was determined by comparing the drug-treated normalized HER2/*neu* transcript signal to that of 4

normalized untreated control HER2/*neu* transcript signals. IC_{50} values for each agent was also determined.

Northern Blot Analysis:

SK-Br-3 cells (5×10^5) were plated in 60 mm dishes. 72 hours after plating, the medium was changed followed by drug addition at the indicated concentrations. At the times indicated after drug treatment, total RNA was harvested from the cells using TRIzol Reagent (GIBCO, Grand Island, NY), as recommended by the manufacturer. Equal amounts (based upon absorbance at 260nm) of total RNA from each sample were electrophoresed for 4.5 hours at 80 volts on a 1.5% agarose-formaldehyde gel (40 mM 3-(N-morpholino)-propanesulfonic acid [pH 7.0], 10 mM sodium acetate, 10 mM ethylenediamine tetraacetic acid and 2.2 M formaldehyde) with a buffer containing 40 mM 3-(N-morpholino)-propanesulfonic acid, pH 7.0, 10 mM sodium acetate, 10 mM ethylenediamine tetraacetic acid. The gel was then transferred overnight to a nylon membrane (Genescreen, NEN Life Science Products, Boston, MA). Following UV cross-linking, the membrane was placed a hybridization bottle with pre-hybridization buffer (0.5 M sodium phosphate, pH 7.2, 7% sodium dodecyl sulfate, 1 mM ethylenediamine tetraacetic acid, 1% bovine serum albumin) at 60°C for 60 minutes. The membrane was then hybridized overnight with [α-^{32}P]-CTP radiolabeled HER2/*neu* cDNA (pBluescript, 1.5Kb *EcoRI* fragment) and [α-^{32}P]-CTP radiolabeled glyceraldehyde 3-phosphate dehydrogenase cDNA (American Type Culture Collection, pBluescript SK$^-$, 1.2Kb *EcoRI* fragment). The hybridized membrane was washed twice for 20 minutes at 60°C with 40 mM sodium phosphate, pH 7.2, 5% sodium dodecyl sulfate, 1 mM ethylenediamine tetraacetic acid, and 0.5 % bovine serum albumin, followed by two additional washes for 20 minutes at 60°C with 20 mM sodium phosphate, pH 7.2, 1% sodium

dodecyl sulfate and 1 mM ethylenediamine tetraacetic acid. Blots were exposed to a PhosphorImaging Screen and the ^{32}P signal of both HER2/*neu* and GAPDH transcript signals were quantitated by a Molecular Dynamics PhosphorImager and analyzed with ImageQuant software. The assessment of drug inhibition of gene expression was determined by dividing the signal of the mRNA bands from drug treated samples by the average mRNA signal generated by 4 untreated control samples.

Results:

Effects of DNA-binding agents on formation of the ESX/HER2/*neu* promoter complex.

DNA-binding agents (structures presented in Figure 1A) with varying binding motifs were evaluated by EMSA for their efficacy at preventing the binding of a purified recombinant Ets protein, ESX, to the HER2/*neu* promoter. An oligonucleotide probe (Figure 1B) containing the EBS consensus-binding site from the HER2/*neu* promoter was incubated with purified ESX and reactions were resolved on a native polyacrylamide gel. A representative EMSA is presented in Figure 2A. Pre-incubating varying drug concentrations with the DNA probe prior to the addition of ESX, as shown for Hoechst 33342 in Figure 2A, inhibited ESX/DNA complex formation in a concentration-dependent manner. For Hoechst 33342 complete inhibition of ESX/DNA complexes was seen at a concentration of 4.0 μM with 50% inhibition at 1.4 μM. Results for each of the DNA-binding agents tested are shown graphically in Figure 2B and their IC_{50} values summarized in Table 1. Comparison of the IC_{50} values of the two A/T preferring drugs, distamycin and Hoechst 33342 (0.7 μM and 1.4 μM, respectively), indicated these agents were similarly effective in preventing complex formation. The G/C preferring intercalator, hedamycin, had the lowest IC_{50} value (0.5 μM) with close to complete inhibition observed at 1.0 μM (Figure 2B). The evaluation of chromomycin A_3 was complicated by the fact that 12 mM Mg^{+2} is needed for optimal chromomycin A_3 binding to DNA and at these levels the ESX/DNA complex was reduced in the absence of drug. A maximal Mg^{+2} concentration of 5 mM was chosen which retained ~60% of the ESX/DNA complex compared with controls without Mg^{+2} (data not shown). These sub-optimal concentrations of Mg^{+2} likely contributed to the relatively high IC_{50} value of 10 μM (as per Table 1A) for ESX/DNA complex inhibition and the fact that it could not

completely inhibit the ESX/DNA complex even up to 20 μM, the highest concentration tested (Figure 2B).

Effects of DNA-binding agents on cell-free expression of HER2/*neu*.

The agents studied in EMSAs were next evaluated for their efficacy as inhibitors of Ets and/or TBP initiated cell-free transcription of the HER2/*neu* promoter template. This assay provides a more complex environment for drug evaluation compared with EMSAs since it includes many other nuclear components and uses a relatively large, linearized plasmid DNA target that contains the HER2/*neu* promoter and luciferase template. Briefly, plasmid was incubated for 1 hour with nuclear extracts from SK-Br-3 cells and [α-^{32}P]-CTP. The radiolabeled transcripts were resolved on a denaturing polyacrylamide gel along with an RNA ladder to identify the major HER2/*neu* band (~760 base pairs) of interest [35].

DNA-binding agents were incubated with the DNA template prior to transcript formation to assess drug effectiveness as an inhibitor of cell-free expression from the HER2/*neu* promoter. Figure 3 shows representative data demonstrating the concentration-dependent inhibition of HER2/*neu* transcript formation by Hoechst 33342. About 95% inhibition of HER2/*neu* transcript formation was observed at 10 μM (lane 2) while detectable inhibition is seen at a concentration as low as 2.5 μM (lane 4). The Hoechst 33342 IC_{50} value in the assay is 3.0 μM (Table 1A). The average levels of inhibition were derived from a quantitative analysis of more than six separate experiments which are not always fully reflected in the individual gel image.

Results of cell-free transcription assays performed for each agent are presented in Figure 4 with IC_{50} values listed in Table 1A. Like the EMSA studies, A/T sequence preferring drugs, distamycin and Hoechst 33342, showed similar IC_{50} values of 3.0 μM (Figure 4). Detectable

inhibition by distamycin was seen at a concentration of 2.5 μM with complete inhibition by 10 μM. Contrary to being the most effective agent in the EMSA analysis, the G/C intercalator, hedamycin, was the least potent inhibitor of cell-free transcription, requiring 25 μM to reach ~90% inhibition. While optimal drug-DNA binding conditions could not be achieved in the EMSAs for chromomycin A_3, the nuclear extract containing transcription conditions, which included higher Mg^{+2} concentrations, likely allowed for more effective binding of chromomycin A_3 to the promoter template. Under these assay conditions, chromomycin A_3 was the most potent HER2/*neu* transcript inhibitor with detectable inhibition by 1.0 μM, an IC_{50} of 1.5 μM and maximal inhibition by 5.0 μM (Figure 5). Consistent with the concentration-dependent decrease in the major HER2/*neu* transcript (760 base pairs), we noted a concentration-dependent drug induced increase in partial transcript production in some samples suggesting an additional effect on transcript elongation (in Figure 3 lanes 2 to 5 the decreased 760 base pair full-length band is accompanied by an increase in partial transcripts located below the 280 base pair marker and just above the internal control in each lane).

Effects of DNA-binding agents on HER2/*neu* cellular mRNA levels in SK-Br-3 cells.

Despite the utility in using simplistic cell-free assays such as EMSA and *in vitro* transcription for evaluating drugs ultimately whole cell assessment is needed to determine their overall effectiveness and target specificity. Northern blot analysis of cells treated 24 hours with each DNA-binding agent was used to determine their ability to inhibit endogenous HER2/*neu* transcription. SK-Br-3 cells, whose viability depends on HER2/*neu* overexpression, were used in these studies. GAPDH (glyceraldehyde 3-phosphate dehydrogenase), a housekeeping gene with comparable mRNA half-life with that of HER2/*neu* mRNA (~8h), was used to measure the

overall effects on the cell's transcriptional machinery [37, 38]. Figure 5A shows a representative Northern blot and the concentration-dependent inhibition of HER2/*neu* mRNA levels by Hoechst 33342. Detectable inhibition was seen at 5.0 μM (lane 4) with a resulting Hoechst IC_{50} of 9.0 μM (Figure 5B and Table 1B). In comparison, GAPDH mRNA was also inhibited to comparable levels as HER2/*neu* following Hoechst 33342 treatment (Figure 5). Northern blots were performed for each of the other drugs (Figure 5) with IC_{50} values presented in Table 1B.

Since cellular uptake and stability may affect drug action and the inhibition of HER2/*neu* and GAPDH transcripts may have different time dependencies, the time-dependent effects on inhibition of mRNA levels were evaluated. The standard assay used a 24-hour time point to allow for the relatively long half-lives of HER2/*neu* and GAPDH. To determine if longer time points might alter the relative transcript inhibiting results, the least cytotoxic agent, distamycin (see Table 1B), was studied since long-term treatment by the other drugs resulted in significant losses in recoverable total RNA. Northern blot analysis was performed on total RNA harvested from SK-Br-3 cells treated with 50 μM distamycin for 24, 48, and 72 hours. As shown in Figure 5 there was a time-dependent decrease in HER2/*neu* mRNA levels that was not significantly different from that of the GAPDH mRNA inhibition.

Effects of DNA-binding agents on SK-Br-3 cell growth.

While all agents tested in Northern blot analysis inhibited HER2/*neu* mRNA production, more than two orders of magnitude differences were observed in drug potency. These differences could result from diverse levels of specificity for the HER2/*neu* promoter or from dissimilar specificities on other essential genes or the general transcriptional machinery. Thus, each agent was evaluated for the ability to inhibit SK-Br-3 cell growth over a 72-hour continuous exposure.

Cell growth inhibition was determined by comparing the cell count of drug-treated samples with the cell count of untreated controls and IC_{50} values are presented in Table 1B. Hedamycin and chromomycin A_3 had IC_{50} values in the sub-micromolar concentration range while the Hoechst 33342 IC_{50} value was in the low micromolar range. Distamycin was clearly the least cytotoxic having an IC_{50} concentration in the hundred-micromolar range. The two agents that were most potent at inhibiting HER2/*neu* and GAPDH mRNA levels, chromomycin A_3 and hedamycin, were also the most potent inhibitors of cell growth. Similarly, for Hoechst 33342 and distamycin, there was a similarity between intracellular mRNA transcription (i.e. Northern blots) and the ability to inhibit cell growth, with Hoechst 33342 being more effective than distamycin in both assays.

Discussion:

Despite understanding the mechanisms by which TFs regulate gene expression at the molecular level, utilization of this information to design inhibitors has lagged. This study assessed the strategy of inhibiting gene expression by targeting DNA binding agents to a transcription factor binding site on a gene promoter in order to disrupt complex formation. Drugs used as gene expression inhibitors are often based upon their inhibitory activity in EMSA assays, which utilizes a purified TF and a small oligonucleotide containing just the TF consensus-binding site. However, results from EMSA studies may not be predictive of drug performance as an inhibitor of expression where regulation involves the interaction of numerous factors within a relatively large gene promoter region. This study not only analyzed drugs for their ability to inhibit the Ets transcription factor, ESX, from binding to its consensus DNA site but also examined whether this ability corresponded to subsequent effects on cell-free and cellular expression of an Ets-regulated gene (HER2/*neu*).

All agents were initially examined in a cell-free EMSA assay and found to inhibit ESX/HER2/*neu* promoter complex formation in a dose-dependent manner with an overall order of potency hedamycin = distamycin > Hoechst 33342 >> chromomycin A_3. Based upon hedamycin's intercalative mode of DNA-binding, its potency as an inhibitor is likely related to its ability to create significant distortion of the DNA helix with loss of binding site recognition by ESX [2, 9, 19, 39, 40]. The minor groove binding agents, distamycin and Hoechst 33342 may also effectively inhibit ESX/HER2/*neu* promoter complex formation by directly competing with ESX for binding to minor groove contacts within its DNA-binding domain. Distamycin's slightly increased efficiency compared with Hoechst 33342, may be due to its capacity to bind as a side-by-side dimer in regions with at least five A/T base pairs resulting in further narrowing of the major groove thus interfering with ESX binding to its major groove contacts [2, 6-9, 41]. Chromomycin A_3 was the least effective inhibitor of ESX/HER2/*neu* promoter complex formation likely due to the use of sub-optimal concentrations of Mg^{+2}, an ion that is required by chromomycin A_3 for DNA-binding. These results contrast with its observed potent inhibition (≤ 1 μM) of other TF/DNA complexes such as early growth response gene-1, Wilms tumor suppressor gene-1 and TATA box binding protein [13].

Whether agents that blocked ESX/DNA complex formation also inhibit Ets-regulated gene expression were evaluated utilizing cell-free expression assays containing an exogenous DNA source in the presence of a nuclear lysate that includes functional transcriptional machinery and endogenous factors including ESX. All agents tested showed a capacity to inhibit cell-free transcription, while in contrast to the EMSA findings, the order of potency of the G/C preferring agents differed, with chromomycin A_3 being the most potent and hedamycin the least: chromomycin A_3 > distamycin = Hoechst 33342 > hedamycin (Table 1A).

Chromomycin A_3's increased efficacy is likely due in part to the enhanced DNA-binding conditions created by the higher concentrations of Mg^{+2} (~7.5 mM), allowing for the formation of the Mg^{+2}-coordinated head-to-tail chromomycin A_3 dimers. That these dimers create significant distortion and opening of the minor groove upon binding to the DNA could contribute to chromomycin A_3's enhanced efficacy [9]. In contrast, hedamycin, a potent inhibitor of ESX/HER2/*neu* complex formation, showed relatively weak inhibition of HER2/*neu* transcript formation. It is not clear why hedamycin's efficacy decreased so dramatically since previously our lab found hedamycin to be an effective inhibition of E2F-dependent cell-free expression [22]. Possibly hedamycin binds at sufficient distances form the transcriptional machinery that the distortion caused by intercalation does not interfere with the transcriptional process. In contrast to chromomycin A_3 and hedamycin, which cause significant helical distortions, distamycin and Hoechst 33342 only produce minimal topological effects on the DNA helix. Distamycin and Hoechst 33342 were equally inhibitory to HER2/*neu* transcript formation and demonstrated limited correlation with the EMSA results. Since these two agents share similar DNA-binding motifs, they would likely target common TF/DNA complexes such as the TATA box binding protein.

From the prospective of the template and transcriptional machinery, inhibition of *in vitro* transcription cannot be attributed exclusively to inhibition of ESX binding since other Ets proteins found in the nuclear extract or other proteins involved in HER2/*neu* regulation could be inhibited. Alternatively, decreased transcription could be due to inhibition of binding by basal transcription factors, such as TATA box binding protein, rather than the prevention of specific Ets protein binding. An effect on general transcriptional machinery rather than targeted inhibition of Ets binding by the MGBs is further supported by the appearance of partial HER2/*neu* transcripts.

Inhibition of cell-free and cellular expression might differ since the latter requires drug access to the nuclear target and stability in a cellular environment. Northern blot analysis revealed a concentration-dependent inhibition of cellular HER2/*neu* mRNA levels with the following potency order: chromomycin A_3 > hedamycin >> Hoechst 33342 >> distamycin. Significantly, only chromomycin A_3 behaved similarly as an inhibitor of cell-free and cellular expression. Also, only the agents inducing significant helical distortions (chromomycin A_3 and hedamycin) were potent inhibitors of cellular HER2/*neu* expression. Drug induced helical distortion could decrease HER2/*neu* transcription by inhibiting the general transcriptional machinery, which is necessary for optimizing expression.

Investigation of drug effects on SK-Br-3 cell growth revealed the same order of potency as observed for northern blot analysis: chromomycin A_3 > hedamycin >> Hoechst 33342 >> distamycin. While the expression data provided fairly specific information about drug effects on a gene target, other non-specific effects in cells can influence cytotoxicity data. For example, the longer time periods utilized in the cell growth inhibition studies will be influenced by drug stability within the cellular environment. In addition, studies have shown some cell lines actively remove Hoechst 33342 [42, 43]. Similarly, cellular uptake might influence cytotoxicity results.

This study revealed the difficulty in extrapolating a drug's ability to inhibit cell-free TF/DNA complex formation to its effectiveness as an inhibitor of both cell-free and cellular gene expression. While each of these assays provide consistent evidence of drug inhibition of TF binding they cannot take into account factors in a whole cell environment that may impinge upon drug activity. Extrapolation of the cellular mRNA inhibition to equally cytotoxic drug levels revealed no agent capable of selectively inhibiting targeted gene expression. Likewise, attempts at correlating TF/DNA complex formation with cellular gene expression and cytotoxicity is difficult

since we cannot ascertain if cell death was due to HER2/*neu* inhibition or to some other drug associated event.

Drug effects on expression in cells may or may not be strictly related to the ability of the drug to target a particular gene promoter. Understanding the mechanism of molecular regulation of a gene promoter and cell-free evaluation of how drugs can affect the individual components of this regulation are needed to develop drugs with enhanced inhibitory activity. There is a need for further development of drugs that cannot only inhibit gene expression in cells, but can do so in a manner that is based upon a DNA targeting strategy. Recent studies have found that uniquely designed sequence specific minor groove binding agents, polyamides, which are not cytotoxic, bind DNA as side-by-side dimers and are extremely effective inhibitors of TF/DNA complex formation and cell-free expression [44-50]. Effective inhibition of ESX binding to the HER2/*neu* promoter as well as inhibition of Ets-regulated cell-free expression by polyamides also was reported [35]. Currently, studies are underway to develop polyamides as more specific inhibitors of HER2/*neu* expression in cells without the accompanying whole-cell cytotoxicity, which often occurs with the more conventional DNA-binding agents.

1. Warings, M.J. and C. Bailly, *DNA recognition by intercalators and hybrid molecules.* Journal of Molecular Recognition, 1994. **7**(2): p. 109-22.
2. Yang, X.L. and A.H. Wang, *Structural studies of atom-specific anticancer drugs acting on DNA.* Pharmacol Ther, 1999. **83**(3): p. 181-215.
3. Neidle, S., *Crystallographic insights into DNA minor groove recognition by drugs.* Biopolymers, 1997. **44**(1): p. 105-121.
4. Chaires, J.B., *Energetics of drug-DNA interactions.* Biopolymers, 1997. **44**(3): p. 201-15.
5. Ren, J. and J.B. Chaires, *Sequence and structural selectivity of nucleic acid binding ligands.* Biochemistry, 1999. **38**(49): p. 16067-75.
6. Pelton, G. and D.E. Wemmer, *Structural characterization of a 2:1 distamycin A d(CGCAAATTGGC) complex by two dimensional NMR.* Proc Natl Acad Sci USA, 1989. **86**: p. 5723-5727.
7. Chen, X., *et al.*, *Binding of two distamycin A molecules in the minor groove of an alternating B-DNA duplex.* Nature Structural Biology, 1994. **1**(3): p. 169-75.
8. Chen, X., B. Ramakrishnan, and M. Sundaralingam, *Crystal structures of the side-by-side binding of distamycin to AT-containing DNA octamers d(ICITACIC) and d(ICATATIC).* Journal of Molecular Biology, 1997. **267**(5): p. 1157-70.
9. Geierstanger, B.H. and D.E. Wemmer, *Complexes of the minor groove of DNA.* Annu Rev Biophys Biomol Struct, 1995. **24**: p. 463-493.
10. Bellorini M, M.V., D'Incalci M, Mongelli N, Mantovani R, *Distamycin A and tallimustine inhibit TBP binding and basal in vitro transcription.* Nucleic Acids Res, 1995. **23**(10): p. 1657-63.
11. Chiang, Y.-S., *et al.*, *Effect of DNA Binding Drugs on EGR1 and TBP Complex Formation with the Herpes Simplex Virus Latency Promoter.* J. Biol. Chem., 1996. **271**: p. 23999-24004.
12. Chiang, S.Y., *et al.*, *Effects of minor groove binding drugs on the interaction of TATA box binding protein and TFIIA with DNA.* Biochemistry, 1994. **33**(23): p. 7033-40.
13. Welch, J.J., F.J. Rauscher, 3rd, and T.A. Beerman, *Targeting DNA-binding drugs to sequence-specific transcription factor/DNA complexes. Differential effects of intercalating and minor groove binding drugs.* J Biol Chem, 1994. **269**(49): p. 31051-8.

14. Gao, X.L., P. Mirau, and D.J. Patel, *Structure refinement of the chromomycin dimer-DNA oligomer complex in solution.* J Mol Biol, 1992. **223**(1): p. 259-79.

15. Sastry, M. and D.J. Patel, *Solution structure of the mithramycin dimer-DNA complex.* Biochemistry, 1993. **32**(26): p. 6588-604.

16. Sastry, M., *et al.*, *Solution structure of the monoalkylated mitomycin C-DNA complex.* J Mol Biol, 1995. **247**(2): p. 338-359.

17. Keniry, M.A., *et al.*, *Nuclear magnetic resonance comparison of the binding sites of mithramycin and chromomycin on the self-complementary oligonucleotide d(ACCCGGGT)2. Evidence that the saccharide chains have a role in sequence specificity.* Journal of Molecular Biology, 1993. **231**(3): p. 753-67.

18. Searle, M., *NMR Studies of Drug-DNA Interactions.* Progress in NMR Spectroscopy, 1993. **25**: p. 403-80.

19. Sun, D., *et al.*, *Structure of the altromycin B (N7-guanine)-DNA adduct. A proposed prototypic DNA adduct structure for the pluramycin antitumor antibiotics.* Biochemistry, 1993. **32**(32): p. 8068-74.

20. Gago, F., *Stacking interactions and intercalative DNA binding.* Methods, 1998. **14**(3): p. 277-92.

21. Neidle S, A.Z., *Structural and sequence-dependent aspects of drug intercalation into nucleic acids.* CRC Crit Rev Biochem, 1984. **17**(1): p. 73-121.

22. Chiang, S.Y., J.C. Azizkhan, and T.A. Beerman, *A comparison of DNA-binding drugs as inhibitors of E2F1- and Sp1-DNA complexes and associated gene expression.* Biochemistry, 1998. **37**(9): p. 3109-15.

23. Snyder, R.C., *et al.*, *Mithramycin blocks transcriptional initiation of the c-myc P1 and P2 promoters.* Biochemistry, 1991. **30**: p. 4290-4297.

24. Ray R, S.R., Thomas S, Koller CA, Miller DM, *Mithramycin blocks protein binding and function of the SV40 early promoter.* J Clin Invest, 1989. **83**(6): p. 2003-7.

25. Miller, D.M., *et al.*, *Mithramycin selectively inhibits transcription of G-C containing DNA.* American Journal of the Medical Sciences, 1987. **294**(5): p. 388-94.

26. White, C.M., *et al.*, *Evaluation of the Effectiveness of DNA-Binding Drugs To Inhibit Transcription Using the c-fos Serum Response Element as a Target.* Biochemistry, 2000. **39**(40): p. 12262-12273.

27. *Ets Gene Family.* Oncogene, 2000. **19**(55): p. 6393-6548.

28. Scott, G., *et al.*, *Ets Regulation of the erbB2 Promoter.* Oncogene, 2000. **19**(55): p. 6490-6502.

29. Klapper, L.N., *et al.*, *Biochemical and clinical implications of the ErbB/HER signaling network of growth factor receptors.* Advances in Cancer Research, 2000. **77**: p. 25-79.

30. Graves, B.J. and J.M. Petersen, *Specificity within the ets family of transcription factors.* Adv Cancer Res, 1998. **75**: p. 1-55.

31. Chang, C.H., *et al.*, *ESX: a structurally unique Ets overexpressed early during human breast tumorigenesis.* Oncogene, 1997. **14**(13): p. 1617-22.

32. Roh, H., *et al.*, *HER2/neu antisense targeting of human breast carcinoma.* Oncogene, 2000. **19**(53): p. 6138-6143.

33. Neve, R., *et al.*, *Biological effects of anti-ErbB2 single chain antibodies selected for internalizing function.* Biochemica & Biophysica Research Communication, 2001. **280**: p. 274-279.

34. Benz, C. and D. Tripathy, *ErbB2 overexpression in breast cancer: biology and clinical translation.* Journal of Women's Cancer, 2000. **2**: p. 33-40.

35. Chiang, S.Y., *et al.*, *Targeting the Ets Binding Site of the HER2/neu Promoter with Pyrrole-Imidazole Polyamides.* Journal of Biological Chemistry, 2000. **275**(32): p. 24246-24254.

36. Scott, G.K., *et al.*, *Binding of an ETS-related Protein within the DNase I Hypersensitive Site of the HER2/neu Promoter in Human Breast Cancer Cells.* J. Biol. Chem., 1994. **269**(31): p. 19848-19858.

37. Dani, C., *et al.*, *Characterization of the transcription products of glyceraldehyde 3-phosphate-dehydrogenase gene in HeLa cells.* European Journal of Biochemistry, 1984. **145**(2): p. 299-304.

38. Pasleau, F., M. Grooteclaes, and R. Gol-Winkler, *Expression of the c-erbB2 gene in the BT474 human mammary tumor cell line: measurement of c-erbB2 mRNA half-life.* Oncogene, 1993. **8**(4): p. 849-54.

39. Henderson, D. and L.H. Hurley, *Specific targeting of protein-DNA complexes by DNA-reactive drugs (+)-CC-1065 and pluramycins.* Journal of Molecular Recognition, 1996. **9**(2): p. 75-87.

40. Pavlopoulos, S., *et al.*, *Structural characterization of the 1:1 adduct formed between the antitumor antibiotic hedamycin and the oligonucleotide duplex d(CACGTG)2 by 2D NMR spectroscopy.* Biochemistry, 1996. **35**(29): p. 9314-24.

41. Wemmer, D., *et al.*, *Minor Groove Recognition of DNA by Distamycin and Its Analogs.*, in *Structural Biology: The State of the Art*, R. Sarma and M. Sarma, Editors. 1994, Adenine Press: Schenectady. p. 301-323.

42. Levina, V.V., E.Y. Varfolomeeva, and M.V. Filatov, *"DNA clearing" from non-covalently bound agents in mammalian cells as a new mechanism of drug resistance.* Membr Cell Biol, 1999. **12**(6): p. 883-93.

43. Filatov, M.V. and E.Y. Varfolomeeva, *Active dissociation of Hoechst 33342 from DNA in living mammalian cells.* Mutat Res Fundam Mol Mech Mutagen, 1995. **327**(1-2): p. 209-215.

44. Dickinson, L.A., *et al.*, *Inhibition of Ets-1 DNA binding and ternary complex formation between Ets-1, NF-kappaB, and DNA by a designed DNA-binding ligand.* J Biol Chem, 1999. **274**(18): p. 12765-12773.

45. Dickinson, L.A., *et al.*, *Anti-repression of RNA polymerase II transcription by pyrrole-imidazole polyamides.* Biochemistry, 1999. **38**(33): p. 10801-7.

46. Dickinson, L.A., *et al.*, *Inhibition of RNA polymerase II transcription in human cells by synthetic DNA-binding ligands [see comments].* Proceedings of the National Academy of Sciences of the United States of America, 1998. **95**(22): p. 12890-5.

47. Gottesfeld, J.M., *et al.*, *Regulation of gene expression by small molecules.* Nature, 1997. **387**(6629): p. 202-5.

48. Bailly, C. and J.B. Chaires, *Sequence-specific DNA minor groove binders. Design and synthesis of netropsin and distamycin analogues.* Bioconjugate Chemistry, 1998. **9**(5): p. 513-38.

49. Chaires, J.B., *Drug--DNA interactions.* Current Opinion in Structural Biology, 1998. **8**(3): p. 314-20.

50. Walker, W.L., M.L. Kopka, and D.S. Goodsell, *Progress in the design of DNA sequence-specific lexitropsins.* Biopolymers, 1997. **44**(4): p. 323-334.

Table 1: IC50 values for each agent tested in cell-free and whole-cell assays. ***A***, the DNA binding agents are listed below with their respective DNA binding properties and IC_{50} values for inhibition of ESX/DNA complex formation in electrophoretic mobility shift assays and HER2/*neu* transcript formation in cell-free transcription assays. ***B***, each agent was evaluated for ability to inhibit HER2/*neu* and GAPDH mRNA production following a 24-hour drug exposure using northern blot analysis. Comparing the cell count of SK-Br-3 cells following a 72-hour continuous drug exposure to the cell count of untreated controls yielded cell growth inhibition values.

A.

Drug	EMSA IC_{50} values (μM)	Cell-free transcription IC_{50} values (μM)
Hoechst 33342	1.4	3.0
Distamycin A	0.7	3.0
Chromomycin A_3	10.0	1.5
Hedamycin	0.5	8.0

B.

Drug	Northern blots (24 hrs) IC_{50} values (μM)		Cell Growth Inhibition (72 hrs) IC_{50} values (μM)
	HER2/*neu*	GAPDH	
Chromomycin A_3	0.04	0.07	0.05
Hedamycin	0.21	0.21	0.10
Hoechst 33342	9	9	7.0
Distamycin A	66	57	114

Figure 1: ***A,*** structures of the DNA binding agents. ***B***, partial HER2/*neu* promoter sequence containing the ESX binding site (bold) and the EBS core sequence (underline). There is also a TBP binding site overlapping the 3'-end of the ESX binding site.

Figure 2: Inhibition of ESX binding to the HER/*neu* promoter by each DNA-binding agents. ***A***, Hoechst 33342 (0-4 μM) was incubated with ^{32}P-labeled oligonucleotide containing a portion of the HER2/*neu* promoter followed by incubation with purified bacterial-expressed ESX protein. Samples were electrophoresed on 4% native polyacrylamide gels, dried, exposed to film and inhibition of ESX/DNA complex formation quantitated by densitometric analysis. The figure shows a representative EMSA demonstrating the concentration-dependent ability of Hoechst 33342 to prevent ESX binding to the HER2/*neu* promoter. ***B***, EMSAs were performed for each agent and the percent inhibition of complex formation was determined by comparing the ESX/DNA complex of drug treated samples to the average complex of 3 untreated controls. The percent inhibition of complex formation was averaged from a minimum of 3 separate experiments and plotted against drug concentration (μM). *Bars*, SD. The IC_{50} values (the amount of drug required to inhibit complex formation by 50%) are summarized in Table 1.

Figure 3: Inhibition of cell-free transcription from the HER2/*neu* promoter by Hoechst 33342. Hoechst 33342 was incubated with linearized plasmid DNA containing the HER2/*neu* promoter followed by incubation with SK-Br-3 nuclear extract and labeling cocktail, as described in Methods. Samples were loaded onto a 7 M-urea polyacrylamide gel, electrophoresed, dried, and exposed to PhosphorImaging Screen with ^{32}P signal quantitated by ImageQuant software. Normalization for equal loading was based on an internal control (IC). The following is a representative cell-free transcription assay showing the concentration-dependent inhibition of HER2/*neu* transcript formation by Hoechst 33342. *Lanes 1, 6, and 7* are untreated controls. *Lanes 2-5* are Hoechst 33342 treatment at 10.0, 5.0, 2.5 and 1.25 μM, respectively. An RNA ladder was used to verify the band of interest based on transcript size, ~760 base pairs, as noted on the scale to the right.

Figure 4: Inhibition of HER2/*neu* promoter transcript expression by each DNA-binding agent. For each DNA binding agent, cell-free transcription assays were performed and the percent inhibition of transcript formation was determined by comparing the normalized HER2/*neu* transcript signal of drug-treated samples with the average normalized HER2/*neu* transcript signal of 4 untreated controls. The percent inhibition of transcript formation was averaged from 3-4 experiments and plotted against drug concentration (μM). *Bars*, SD.

Figure 5: Inhibition of HER2/*neu* cellular mRNA levels in SK-Br-3 cells by DNA-binding agents. ***A***, SK-Br-3 cells were exposed to Hoechst 33342 for 24 hours at the indicated concentrations followed by harvesting total RNA. Samples were electrophoresed on a formaldehyde-agarose gel, transferred to nylon membrane and probed with GAPDH and HER2/*neu* ^{32}P-labeled cDNAs. Shown is a representative northern blot demonstrating a concentration-dependent decrease in HER2/*neu* and GAPDH mRNA signals produced by Hoechst 33342. *Lanes 1, 2, 7 and 8* are untreated controls, *Lanes 3-6* are Hoechst 33342 treatments at 10, 5.0, 2.5 and 1.0 μM, respectively. ***B***, Northern blot analysis of cells treated 24 hours with each agent was performed and the percent inhibition of mRNA production determined for both HER2/*neu* (■) and GAPDH (◪). Comparison of the drug treated HER2/*neu* signal to the average HER2/*neu* signal of 4 untreated controls yielded percent inhibition of mRNA production. The results were averaged from a minimum of 2 experiments with duplicate samples and plotted against drug concentration. Additionally, northern blot analysis was performed after continuous 50 μM distamycin treatment of SK-Br-3 cells for 24, 48 and 72 hours. Comparison of distamycin-treated mRNA signal to the average signal generated by 4 untreated controls yielded percent inhibition HER2/*neu* and GAPDH mRNA production. The results of 6 separate studies were plotted against time. GAPDH mRNA was used in this study as a measure of general transcription versus HER2/*neu* mRNA as the drug-targeted site of transcription. Equal loading was verified by visual inspection on a UV light box. For some data points error bars were not included since RNA recovery made it difficult to obtain consistent data. The difficulty occurred because the drug was relatively cytotoxic under the conditions studied. *Bars*, SD.

Figure 1

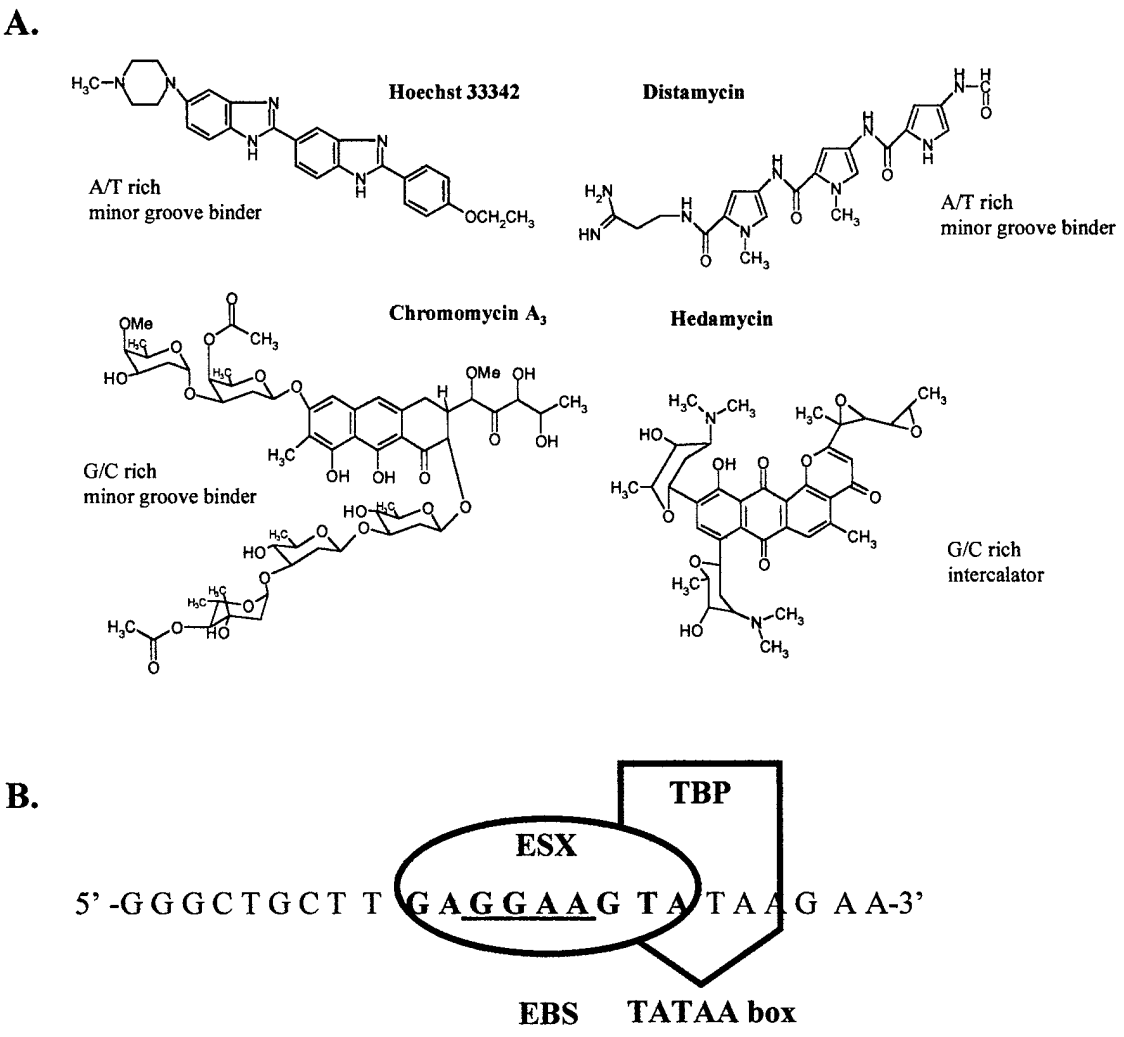
A.
Hoechst 33342
A/T rich
minor groove binder
Distamycin
A/T rich
minor groove binder
Chromomycin A3
G/C rich
minor groove binder
Hedamycin
G/C rich
intercalator
B.
TBP
ESX
5' -G G G C T G C T T G A G G A A G T A T A A G A A-3'
EBS
TATAA box

Figure 2

A.

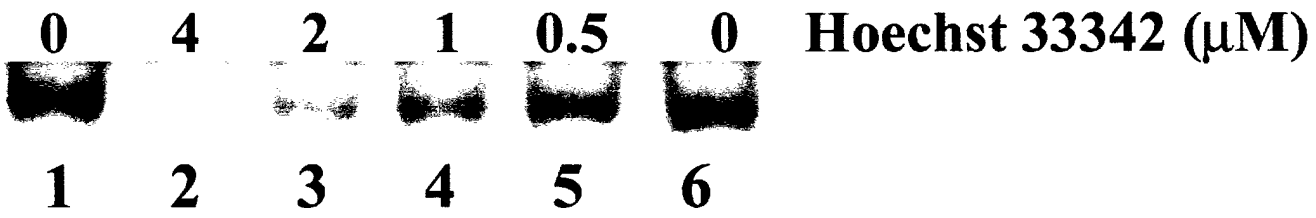
0
4
2
1
0.5
0
Hoechst 33342 (μM)
1
2
3
4
5
6

B.

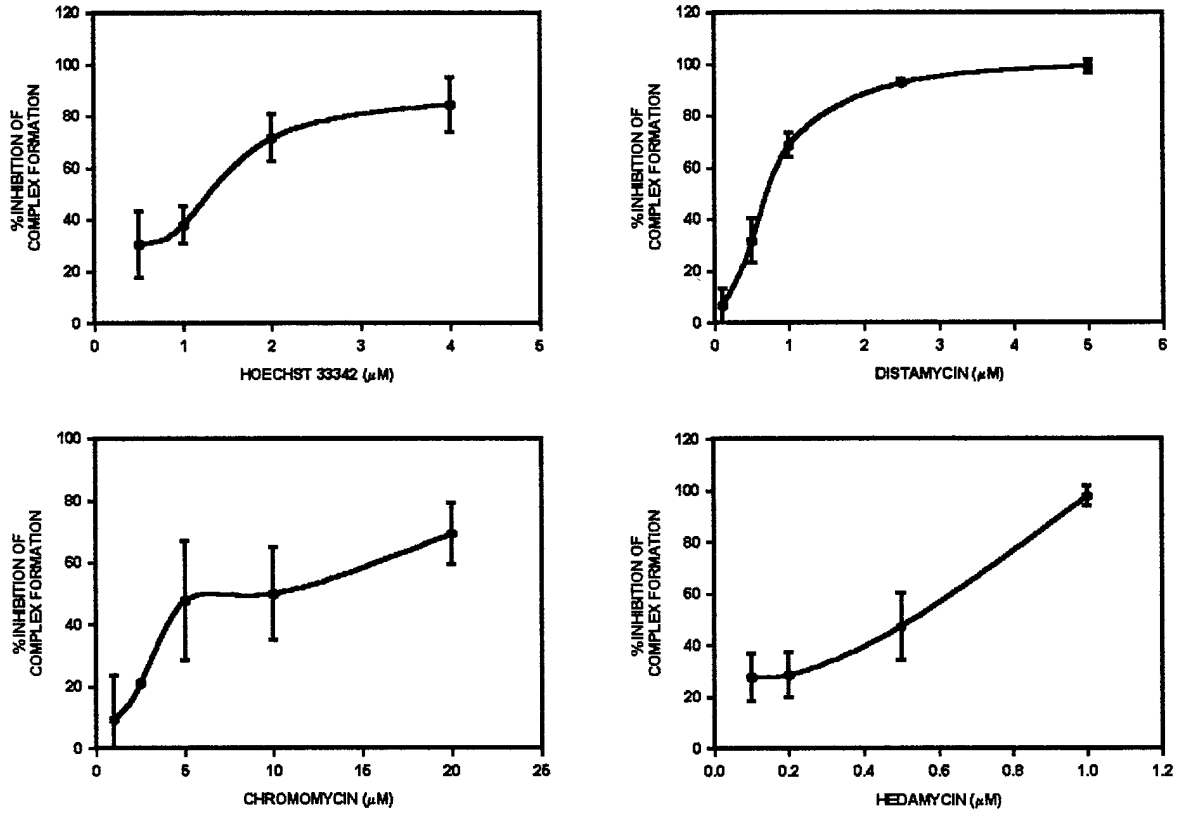
%INHIBITION OF COMPLEX FORMATION
HOECHST 33342 (μM)
DISTAMYCIN (μM)
CHROMOMYCIN (μM)
HEDAMYCIN (μM)

Figure 3

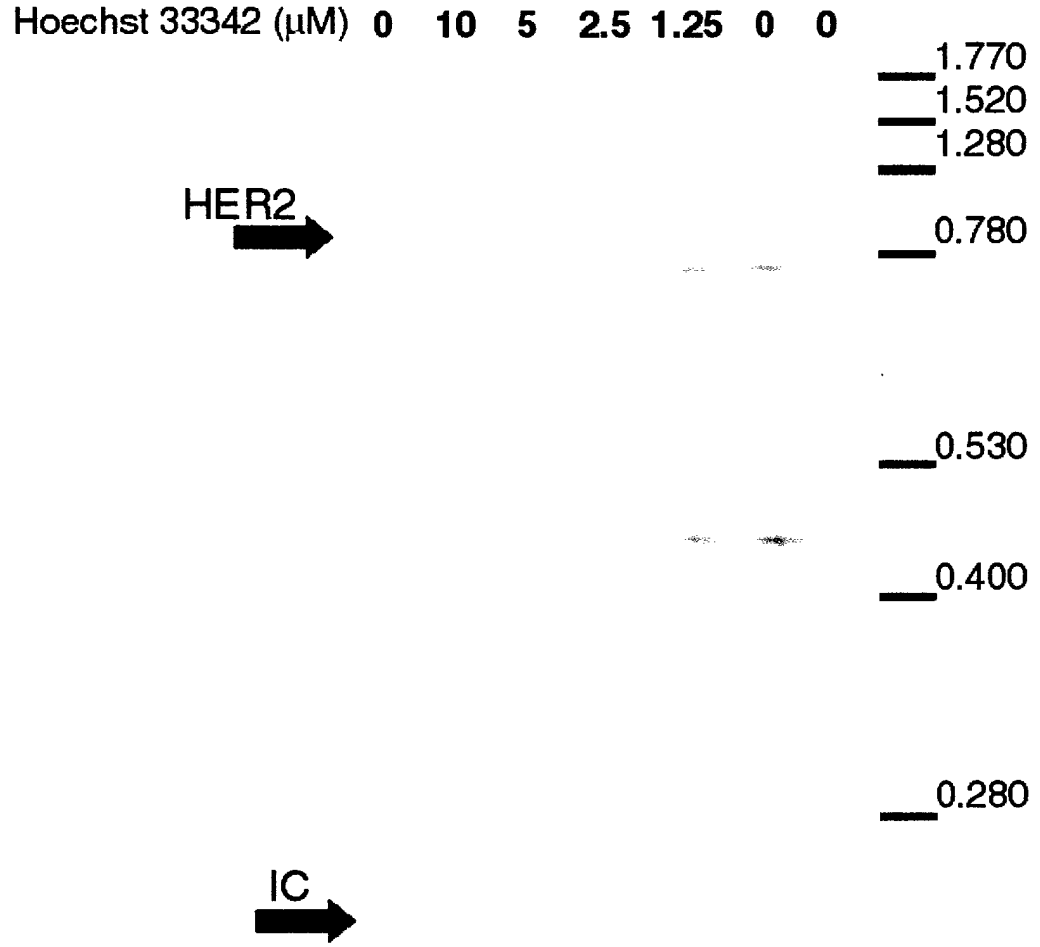
Hoechst 33342 (μM) 0 10 5 2.5 1.25 0 0
1.770
1.520
1.280
HER2
0.780
0.530
0.400
0.280
IC
1 2 3 4 5 6 7

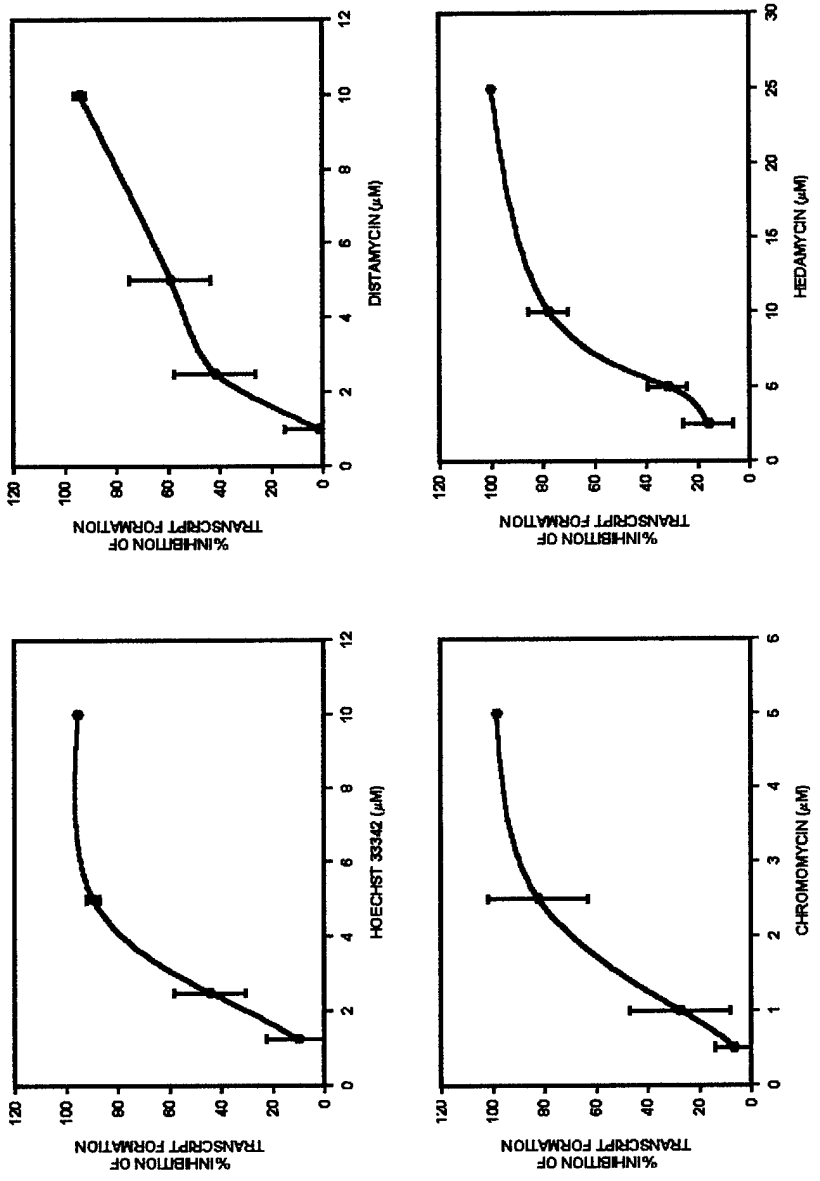
% INHIBITION OF TRANSCRIPT FORMATION
DISTAMYCIN (μM)
HEDAMYCIN (μM)
HOECHST 33342 (μM)
CHROMOMYCIN (μM)

Figure 4

Figure 5

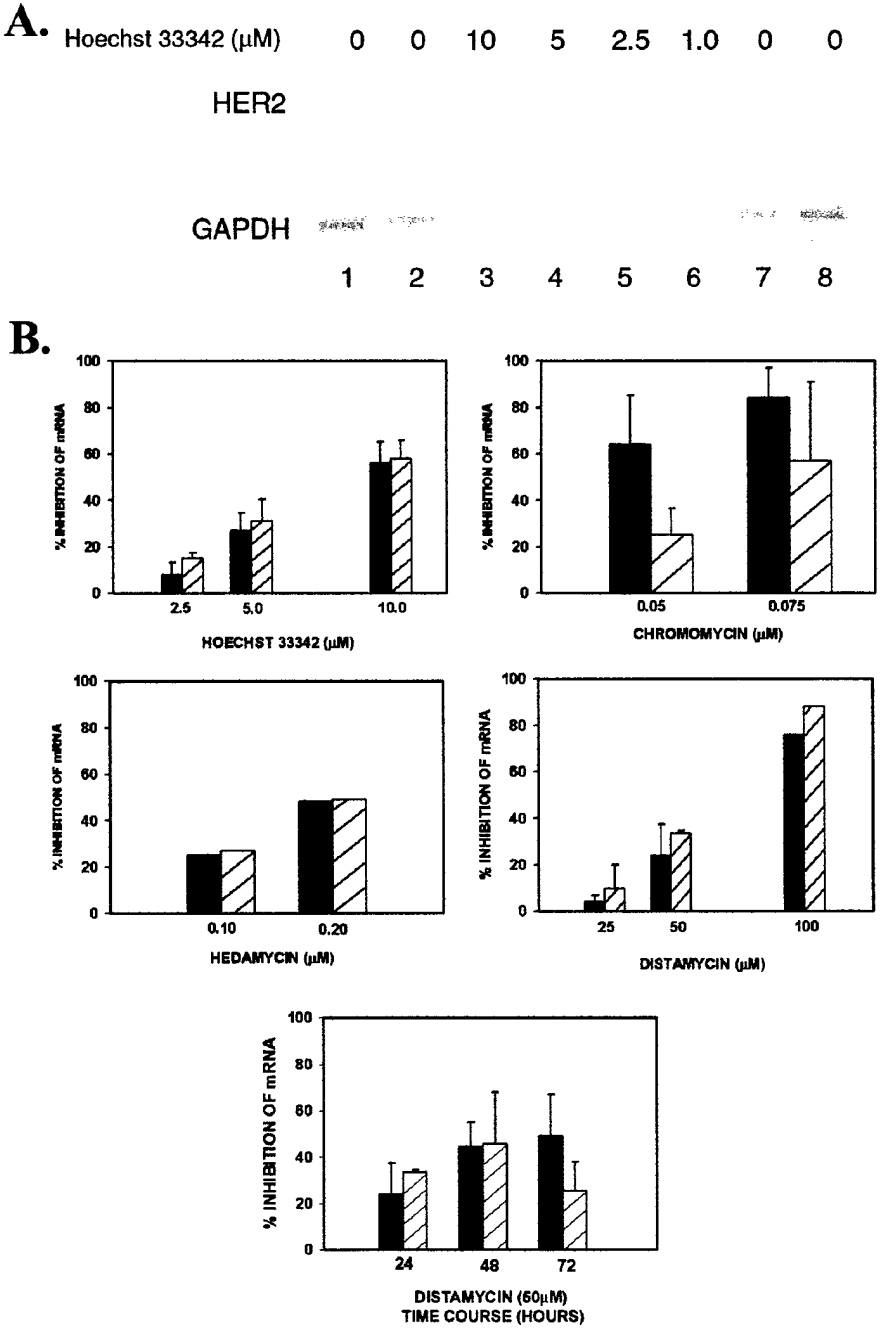
A.
Hoechst 33342 (μM) 0 0 10 5 2.5 1.0 0 0
HER2
GAPDH
1 2 3 4 5 6 7 8
B.
% INHIBITION OF mRNA
HOECHST 33342 (μM)
CHROMOMYCIN (μM)
HEDAMYCIN (μM)
DISTAMYCIN (μM)
DISTAMYCIN (60μM)
TIME COURSE (HOURS)

Appendix C

Manuscript #2

"Polyamide 22, a sequence specific DNA-binding ligand is sequestered in the cell nucleus following uptake in SKBR3 human breast cancer cells."

Title: Polyamide **22**, a Sequence Specific DNA Binding Ligand is Sequestered in the Cell Nucleus Following Uptake in SKB3 Human Breast Cancer Cells.

Authors: Stephanie J. Leslie, Roland W. Bürli, Suryanarayan Somanathan, Ronald Berezney, Peter B. Dervan[2] and Terry A. Beerman[2].

Department of Pharmacology and Therapeutics, Roswell Park Cancer Institute, Buffalo, NY 14263 [S.J.L, T.A.B]; Division of Chemistry and Chemical Engineering and Beckman Institute, California Institute of Technology, Pasadena, California 91125 [R.W.B., P.B.D]; Biological Sciences, State University of New York at Buffalo, Buffalo, NY 14260 [S.S., R.B.]

Running Title: Sequestering of polyamide 22 in the cell nucleus

Key Words: polyamides fluorescence permeability localization nuclei

Footnotes:

[2] To whom correspondence and reprint requests should be addressed: Terry Beerman, Department of Pharmacology and Therapeutics, Roswell Park Cancer Institute, Elm and Carlton Streets, Buffalo, New York 14263. Tel: 716-845-3443; Fax: 716-845-8857; e-mail terry.beerman@roswellpark.org. and Peter Dervan, Division of Chemistry and Chemical Engineering and Beckman Institute, California Institute of Technology, Pasadena, California 91125. Tel: 626-395-6002; Fax: 626-683-8753; e-mail: dervan@cco.caltech.edu.

Abstract:

Polyamides, a new class of sequence specific DNA minor groove binding compounds were evaluated for their permeability to intact cells. Polyamide **2**, a compound originally designed to target the ETS transcription factor DNA binding domain within the HER2/neu promoter, was modified by the addition of a bodipy fluorescent tag to create polyamide **22**. The fluorescent **22** displayed similar DNA binding characteristics as the parent compound. Following addition of **22** to a human breast cancer cell line SKBR3, quantitation by spectrofluorophotometric analysis revealed that up to 25 percent of the compound entered the cell. Fluorescence microscopy demonstrated that **22** was rapidly taken up by cells and by 15 minutes it was localized almost exclusively in the nucleus while avoiding the nucleoli. When cells were incubated with bodipy alone, fluorescence was only seen in the cytoplasm, suggesting that the nuclear signal observed with the **22** treatments was not caused by release of the tag prior to polyamide entry into the cell. Polyamide **22** could be competed by the parent compound and only minimally or not at all with other minor groove binding agents. Fluorescence intensity was also reduced when cells were treated first with **22** for four hours followed by a 6 hour chase using a high concentration of **2**. The pattern of **22** localization when compared to other DNA minor groove binding agents closely resembled Hoechst 33342 and DAPI which are widely used to stain the overall chromatin inside the cell nucleus. High resolution confocal microscopy confirmed the sequestering of polyamide **22** in the extranucleolar regions of the cell nucleus and revealed staining patterns that resembled higher order chromatin domains.

Introduction

Polyamides represent a novel class of DNA binding ligands that makes it possible to target unique DNA sequences (1-3). These agents bind the minor groove of DNA as anti-parallel side by side dimers with binding constants in the 10^{10} range for high binding affinity binding sites (1, 4). Sequence recognition of all four DNA bases is achieved by positioning an N-methylimidazole opposite guanine or N-methylpyrrole opposite cytosine as well as an N-methylpyrrole or hydroxymethyl pyrrole opposite adenosine or thymidine respectively (5). By linking DNA recognition elements with an appropriate hairpin turn to accommodate dimer binding, polyamides can be directed to a specified DNA sequence up to 16 base pairs in length (6). The exquisiteness of the DNA recognition, is illustrated by the finding that a one base mismatch between a polyamide and its DNA binding site results in over an order of magnitude decrease in binding affinity (7).

While the chemistry of polyamide recognition of DNA has been pursued in depth, utilization of these agents on biological targets is just beginning. Recent studies demonstrate that it is possible to inhibit transcription factor DNA complexes by directing polyamides to the binding site of the transcription factor DNA binding domain (8, 9). In the case of polyamides directed towards the TFIIIA DNA binding site within the promoter region of the 5S RNA gene, inhibition of complex formation was accompanied by a loss of gene expression (10). Other studies demonstrate that a rationally designed polyamide could interfere with binding of early protein 2 to its cognate binding site within the cis recognition sequence of the cytomegalovirus major immediate early promoter (8). Further versatility of polyamides as DNA targeting agents are revealed in studies that show inhibition of targeted genes in intact cells. For polyamides directed towards the 5S RNA promoter, patterns of inhibition of 5S RNA gene expression were similar whether treatment was under cell free conditions or carried out with intact cells (10). In another study, viral replication was strongly inhibited in cells treated with polyamides synthesized for binding to RNA polymerase II promoters of genes needed for HIV type 1 RNA synthesis (11).

The cited examples provide indirect evidence that polyamides can work in a cellular environment, but the findings do not directly assess some fundamentally important features about polyamides, such as their ability to be taken into cells and where localization might occur. In general, minor groove binding agents show differing ability to be taken up by cells and also where they bind varies. The classic minor groove binding compound Hoechst 33258 binds to both DNA and RNA and is found in the cell nucleus as well as in the cytoplasm (12). In comparison a structurally similar molecule Hoechst 33342 enters cells even more readily and is found almost exclusively within the cell nucleus (12).

To address the question of how polyamides compare to classical minor groove binding agents in regard to cellular uptake and localization, a polyamide containing a fluorescent Bodipy tag was synthesized (**22**) so it could be tracked within cells. This compound was a modification of **2** a polyamide under study as an inhibitor of the binding of the ETS protein ESX to a regulatory sequence within the proximal promoter of the HER2/neu oncogene (13-15). The fluorescent **22** was compared to the parent compound to show that the addition of the Bodipy does not significantly alter the properties of the polyamide in regard to DNA binding and inhibitory activity on gene expression. Analysis of **22** uptake was carried out using the human breast cancer cell line SKBR3, which overexpress HER2/neu, the target of the parent polyamide **2** (16). A quantitative assessment of ligand uptake was determined from spectrofluorophotometric measurements on **22** treated cells, while a qualitative analysis was made by examining cells under a fluorescence microscope. Uptake was determined both as a function of **22** concentration and time, while assessment of localization was made using both standard epifluorescence and high resolution confocal microscopy. The study demonstrates that polyamide **22** readily enters mammalian cells and localizes predominantly in the extranucleolar regions of the cell nucleus.

Materials & Methods:

Cells:

SKBR-3 cells were obtained from ATCC (Rockville, MD). Cells were grown in McCoy's 5a medium (GIBCO, Grand Island, NY) with 10% fetal bovine serum and cultured at 37°C with 5% CO_2. Normal human diploid fibroblasts (neonatal skin cells where a gift from Dr. Jane Clifford)

were grown in DMEM supplemented with 0.5 mM sodium pyruvate, 1% L-glutamine and 10% fetal bovine serum and cultured at 37°C with 10% CO_2.

Ligands:

Drugs:

Stocks of Hoechst 33342 (Sigma), Hoechst 33258 (Sigma), and DAPI (Boehringer Mannheim) were prepared in ddH_2O.

Synthesis:

Footprint analysis:

MSA:

Mobility shift assays, as described previously, were used to detect differences in the biological activity between the ligands as determined by their effectiveness in preventing transcription factor protein binding to DNA (14). Briefly, an oligonucleotide the ESX consensus binding site (polyamide targeted sequence) from the HER2/neu promoter was incubated with purified ESX (30 minutes at room temperature) and reactions were resolved on a native polyacrylamide gel. A ligands's ability to prevent ESX/DNA complexes was assessed by a 30-minute incubation of the oligonucleotide and the drug prior to the 30-minute incubation with ESX protein. Using Molecular Dynamics ImageQuant software, rectangles were drawn around the ESX/DNA band and the density determined for controls and ligand treated samples. Percent of the control complex formed was determined by comparing the signal of the ESX/DNA band of ligand treated samples by the average signal generated by 4 untreated control ESX/DNA bands.

Spectrofluorophotometer studies:

SKBR3 cells were plated in 60mm dishes at a sub-confluent density of 5×10^5 cells/dish. 72 hours after plating, the cells entered log phase and the media was changed followed by addition of polyamide **22** at 0.5 μM for 15 minutes, 1 and 4 hours. Cells were washed in PBS, trypsinized and pelleted. Cells pellets were then washed 3X in PBS, resuspended in lysis/extraction buffer containing 0.3N HCl: 96% EtOH (1:1) and incubated overnight at 4°C. Following collection of supernatant by centrifugation, fluorescent signal was read on a Shimadzu recording spectrofluorophotometer model RF-540 at the following parameters: excitation wavelength of 504 nm and emission wavelength of 512 nm. Standard curves of free polyamide **22** were

prepared in the same lysis/extraction buffer and were utilized for determining amount of recovered polyamide **22** from the cells.

Epifluorescence Microscopy:

SKBR3 cells were plated at $1x10^4$ cells (in 100µl) on a flame sterilized coverslip (No.1, 22x22) and allowed to adhere for 1 hour at 37°C with 5% CO_2, prior to the addition of 1ml of media. 72 hours after plating, ligand or drug was added at the indicated concentrations and times. Harvesting of the coverslips were carried out in the dark following treatment. Coverslips were PBS washed 3X, fixed in ice-cold acetone for 15 minutes, followed by rehydration in ice-cold PBS for an additional 15minutes. Coverslips were then rinsed in water and mounted (GelMount, Fisher) on a slide. Slides were visualized on an Olympus BX-40 epifluorescent microscope, NB filter (for polyamide **22**), WIY filter (for Hoechst 33342, Hoechst 33258 and DAPI) and images captured using an attached Kodak EOS-DCS5 digital camera.

Confocal Microscopy:

Slides were prepared as described above and examined under a Biorad MRC-1024 confocal microscope system equipped with a krypton-argon laser and Nikon (Optophot™) microscope. The objective was a Zeiss 60X oil immersion planApo with a 1.4 numerical aperture and the 488 nm emission band from the krypton-argon laser was used for excitation of the bodipy fluorochrome. Optical sections of 512 x 512 pixels x 8 bits/pixel were collected through the samples at 0.5 um intervals.

RESULTS:

Effects on ligand binding to DNA following the addition of the fluorescent tag, Bodipy.

While the DNA footprint analysis revealed that polyamide **22** recognition and binding activity was not severely altered by the presence of the fluorescent tag, mobility shift assays (MSAs) were employed to compare each ligand's biological activity, in regard to preventing ESX/DNA complex formation. Briefly, an oligonucleotide containing the targeted ESX consensus-binding site from the HER2/neu promoter was incubated with purified ESX (30 minutes at room temperature) and reactions were resolved on a native polyacrylamide gel. Binding of ESX to the oligo resulted in a slower migrating ESX/DNA band compared to free oligo. Ligand activity in preventing ESX/DNA complex formation was determined by incubating the ligand with the oligo (30 minutes at room temperature) prior to the addition of ESX and an additional 30-minute incubation period. The percent of ESX/DNA complex formation compared to control was determined for each polyamide concentration and the results are shown in Figure 2B. Polyamide **2** at 10 nM resulted in a 40% reduction of complex formation compared to non-ligand treated controls and at 25nM further reduced complex formation. On the other hand, treatment with polyamide **22** at 30 nM resulted in no detectable reduction compared to control, however, at 50 nM, polyamide **22** reduced complex formation by ~50%. These MSA results indicated a 3-fold difference between polyamides **2** and **22**'s ability to bind the oligonucleotide and prevent ESX/DNA complex formation. Moreover, each ligand was also tested in a cell-free transcription assay and demonstrated that polyamide **22** was 3-fold less active than polyamide **2** at inhibiting HER2/neu transcript production (data not shown).

Polyamide 22 uptake in SKBR3 cells.

The cell-free results suggest that the fluorescently labeled polyamide had the same sequence preference and similar biological activity, albeit slightly decreased, to the parent compound, polyamide **2**. Hence, polyamide **22**, is a reasonable representative model for polyamides in whole cells studies, and with its fluorescent tag, readily available for determining cellular uptake of these types of agents, which is still unclear. For these studies we utilized the SKBR3 cell line, which over-express HER2/neu (the polyamide targeted sequence) and exposed them to polyamide **22** at 0.5 μM for various times. The fluorescent signal of the supernatant

from lysed cells was measured on a spectrofluorophotometer at an excitation wavelength of 504 nm and emission of 512 nm. The amount of recovered polyamide **22** from cells was determined by comparison to a standard curve of the fluorescent signal of free polyamide **22**. The results, shown in Figure 3, indicate that the cells took up the ligand in a time dependent manner; with ~15% of the polyamide treatment taken up within 15 minutes and a further increase up to ~30% by 4 hours.

Polyamide 22 localization in SKBR3 cells.

While the spectrofluorophotometer results indicate that the cells take up the ligand, it does not indicate location within the cells. To evaluate localization of **22**, epifluorescent microscopy studies were undertaken. Briefly, SKBR3 cells that were grown on glass coverslips were exposed to polyamide **22** at 0.5 μM for 4 hours then washed several times with PBS, followed by fixation in acetone, re-hydration in PBS, rinsed and mounted to slides prior to viewing on an epifluorescence microscope. The results are shown in Figure 4 using two images. Figure 4A is the phase/contrast image for visualization of cytoplasmic boundaries, nuclei and nucleoli in the nuclear interior, while Figure 4B is the fluorescent image of the same field. The fluorescently tagged polyamide **22** is localized primarily in the nucleus with avoidance of the nucleoli, the dark structures identified by the black arrows in Figure 4A and the corresponding white arrows in 4B. The finding that fluorescence was detected only in the cytoplasm of cells treated with bodipy alone (Figure 4C and D) suggest that the nuclear fluorescence was due to polyamide **22** localization and not a consequence of breakdown of the ligand and subsequent movement of bodipy into the nucleus.

Time study of polyamide 22 uptake and localization.

The spectrofluorophotometer studies detected a slight increase in cellular uptake over time (Figure 3) and the initial fluorescence microscope studies demonstrated nuclear localization, at least for the 4 hour time point examined. Time course studies were carried out to determine cellular distribution of polyamide **22** over time. SKBR3 cells were exposed to polyamide **22** at 0.5 μM from 5 minutes up to 24 hours and the results are shown in Figure 5. At the earliest time point of 5 minutes, fluorescence was detected, albeit weakly, in the cell nucleus with little or no detectable staining in the cytoplasm. The intensity of nuclear fluorescence increased rapidly for

up to one hour and then increased more gradually up to 24 hours (Figure 5). At all time points little or no cytoplasmic fluorescence was detected. These results are consistent with the spectrofluorophotometric measurements shown in Figure 3 and further demonstrate that the progressive increase in fluorescence with time is predominantly due to a corresponding accumulation of polyamide **22** in the nucleus. Similar results were obtained when polyamide 22 was incubated with a normal human diploid cell line (NHDF 4085) (results not shown) indicating that the results obtained with the SKB3 human breast cancer cells are generally characteristic of polyamide 22 localization in mammalian cells.

Polyamide 2 competition with polyamide 22 for cellular uptake and binding.

Competition and chase studies utilizing polyamide **2** were performed to investigate the possibility that the presence of the fluorescence tag influenced the cellular uptake and localization. If polyamide uptake and localization is independent of the fluorescent tag than the parent compound should be able to compete for cellular uptake, which would be detected by a decrease in fluorescence. Competition studies utilized SKBR3 cells grown on coverslips treated with either polyamide **22** alone at 0.5 μM (Figure 6A) or polyamide **22** with 10-fold excess of polyamide **2**, (0.5 μM and 5.0 μM, respectively; Figure 6B). In the presence of polyamide **2**, detectable fluorescence was significantly decreased compared to polyamide **22** alone. Moreover, competition studies with increasing amounts of polyamide **2** resulted in a further decrease in fluorescence signal to barely detectable levels (data not shown).

If binding in the nucleus is independent of the presence of the fluorescent tag than polyamide **2** should be able to bind to the same target, effectively chasing the polyamide **22** from the binding site. Chase studies employed a 4-hour pre-treatment of cells with polyamide **22** at 0.5 μM followed by a 6-hour chase by either water (Figure 6C) or polyamide **2** at 5.0 μM (Figure 6D). These results also showed a significant decrease in fluorescence when polyamide **2** was present.

Comparison of polyamide 22 with other DNA minor groove binding agents for localization and staining in SKBR3 cells.

Polyamides are designed to bind to DNA and the epifluorescence microscopy results suggest that polyamide **22** may be reaching its target in the nucleus, while avoiding, the nucleoli, a site concentrated in RNA. Comparison of polyamide **22** localization and binding patterns to the patterns of other known DNA minor groove binding agents may suggest the molecular binding site of the polyamides. DNA minor groove binding agents chosen for these studies include Hoechst 33342, Hoechst 33258 and DAPI, which have known fluorescent properties and have been well studied for cellular localization (17). SKBR3 cells were grown on coverslips, exposed to each agent for 1 hour, harvested and visualized as described in Material and Methods. The results are shown in Figure 7 with the phase/contrast images on the left-hand side and the fluorescent signal of the same field on the right-hand side. Comparison of the two images illustrates the localization patterns of each agent. Figure 7A and B is the result of a polyamide **22** treatment at 1 μM, and displays the ligand's nuclear localization accompanied by avoidance of the nucleoli. Hoechst 33342 (Figure 7C and D) and DAPI (Figures 7G and H) showed a similar extranucleolar pattern of fluorescence in the nucleus with little or no detectable cytoplasmic staining. In contrast, Hoechst 33258, which has almost identical structure and fluorescent properties to Hoechst 33342 but readily binds to RNA as well as DNA, resulted in visible cytoplasmic staining (red/orange) with a significantly decreased nuclear fluorescence compared to Hoechst 33342 (Figure 7E and F). We conclude that polyamide **22** localizes to the cell nucleus of mammalian cells much like the classic DNA specific minor groove binding agents Hoechst 33342 and DAPI which are widely used to stain the overall chromatin pattern inside the cell nucleus. Thus polyamide **22** also stains the overall chromatin in the nucleus.

Laser scanning confocal microscopy following treatment with polyamide 22.

To confirm and extend the epifluorescence microscopic studies we performed time studies of polyamide uptake using laser scanning confocal microscopy. Representative midplane optical sections following incubation of SKBR3 cells with polyamide **22** between 4 to 28 hours are shown in Figure 8. The results conclusively demonstrate that the polyamide **22** is virtually exclusively targeted to the extranucleolar regions of the cell nucleus with no detectable cytoplasmic staining over the time span examined. The multiple nucleolar regions, characteristic of cancer cells, are clearly seen as the very large black areas devoid of fluorescence. Interestingly, a fine granular pattern of staining is often detected (see, e.g, Figure 8B), that may

reflect higher order arrangement of the chromatin domains stained by polyamide **22**. Arrangement of the granular-like stained structures into higher arrays of structures is also suggested around the nucleolar regions, along the nuclear periphery and in various other extranucleolar regions inside the cell nucleus (see e.g., Figure 8B).

Discussion.

Polyamides are a conceptually new form of DNA minor groove binding agent, which through modular design can achieve a remarkable degree of sequence recognition (1). Numerous papers have been published on the chemistry describing how polyamides can be designed to recognize unique sequences of DNA based upon selective binding motifs to all four DNA bases, although relatively little is known about the ability of these agents to target biological molecules in cells (2, 5, 18). While there are several examples of cells treated with polyamides resulting in inhibition of gene expression there is no direct evidence that these agents are taken up by cells (9, 10). This study is the first to track the uptake of a polyamide into a cell and to determine its distribution.

To determine uptake, a well characterized polyamide, **2** originally designed to target a DNA sequence within the HER2/neu promoter was tagged with fluorescent Bodipy. Based upon spectrofluorophotometric analysis of SKBR3 cells treated with **22**, significant uptake occurs within 15 minutes and by four hours about 25 % of the compound is taken up (Fig. 3). Microscopic analysis of these cells revealed that by 15 minutes much of the drug was localized within the nucleus and by four hours compound in the cytoplasm was barely detectable (Fig. 5). The appearance of the fluorescent signal in the nucleus was not the result of degradation of **2** and the subsequent release of free tag, since bodipy alone only localizes to the cytoplasm (Compare Figs. 4A&B with C&D). It was also found that uptake was temperature dependent and that incubations at 4° resulted in no detectable uptake into the cell (data not shown). Finally, a similar profile of **22** uptake into normal human diploid fibroblasts cells was seen, demonstrating that polyamide permeability into mammalian cells is not limited to the neoplastic SKBR3 cell type (Leslie and Beerman, unpublished observation).

The observation that treatment with a 10:1 mixture of the nonflourescent **2** and **22** respectively markedly reduced the fluorescence signal intensity suggests that both agents share a common uptake pathway and that the presence of the Bodipy tag is likely not altering the

mechanism for cellular uptake and retention. Studies showing that **2** can chase the fluorescent **22** signal indicate that the parent and fluorescent compound have similar nuclear binding sites. The poor ability of a conventional DNA minor groove binding agent Hoechst 33342 to chase the **22** signal from the nucleus could indicate that the strong DNA binding properties of polyamides are a factor in where these molecules bind (data not shown) and are retained inside the cell nucleus.

Polyamide **22** shows a characteristic pattern of strong signal throughout the nucleus with the exception that almost no fluorescence is observed within the nucleolus region (Fig. 4A/B). This compares quite well to the uptake patterns for both Hoechst 33342 and another minor groove binding agent DAPI (Fig. 7) which are widely used for staining the overall chromatin inside the cell nucleus. In contrast, Hoechst 33258, which differs from Hoechst 33342 by the substitution of a ethoxy group for the hydroxyl group on the phenol ring, shows a very limited amount of uptake within the nucleus (12, 19). It has been reported that the 33342 Hoechst and DAPI bind almost exclusively to DNA within the nucleus while the 33258 compound can bind to RNA and DNA and is taken up both into the nucleus but even more strongly into the cytoplasm (12). Similarly, the levels of uptake between the two Hoechst compounds varies, with 33342 being much more efficiently taken up (three fold) by mammalian cells (20). At this point, it is not known whether other types of polyamides will possess the uptake characteristics and nuclear localization patterns of **22** which is like Hoechst 33342 or that variants will be seen such as those that whose binding is reminiscent of Hoechst 33258 or potentially other patterns of distribution.

Laser scanning confocal microscopic analysis enabled us to more precisely visualize the intranuclear pattern of polyamide **22** fluorescence. The results illustrated in Figure 8 confirm the extranucleolar localization in the nucleus and the absence of detectable signal in the cytoplasm. Moreover the overall nuclear staining pattern of the chromatin appears as granular-like structures that appear to be arranged in higher order arrays that often surround the nucleolus, nuclear periphery and in various other regions in the nuclear interior. Further studies of these putative granular-like structures decorated by polyamide **22** are being planned using computer imaging segmentation and three-dimensional computer imaging approaches. Preliminary measurements indicate that the repeating chromatin structures have x-y dimensions of about 0.5 microns (Berezney and Somanathan, unpublished findings). This is in the same size range as the replication/transcription sites detected in mammalian cells. Previous studies have further indicated that replication sites are characteristic features of higher order chromatin domains.

Thus the staining patterns of polyamide **22** may be revealing a fundamental aspect of higher order chromatin organization and function in the cell nucleus.

While the initial purpose of this study was to identify where a polyamide resides in mammalian cells, some of the features of the localization suggest that the unique sequence specific nature of the polyamides may be a useful approach for designing compounds that bind to specific regions of functional chromatin. Moreover these compounds offer the potential for direct visualization of such functional elements as origins of DNA replication or promoter sites of transcription within the nucleus of the intact cell.

Figure Legends:

Figure 1. Creation of the fluorescently labeled polyamide, 22. Polyamide **22** was created by the addition of Bodipy to polyamide **2**.

Figure 2B. Comparison of 2 and 22 biological activity using a mobility shift assay. Polyamides **2** (■) and **22** (▨) were incubated with an oligonucleotide containing the targeted ETS binding sequence from the HER2/neu promoter for 30 minutes at room temperature followed by an additional 30 minutes incubation with purified ESX protein. Reactions were resolved on a 4% native polyacrylamide gel and the percent of control ESX/DNA complex formation was determined.

Figure 3. Spectrofluorophotometric determination of polyamide 22 uptake into cells. SKBR3 cells were treated with **22** at 0.5 μM for the indicated times. Cells were then washed, trypsinized and the cell pellets washed 3X in PBS. Pellets were then resuspend in lysis/extraction buffer and incubated overnight at 4°C. The supernatant was collected following centrifugation, fluorescent signal quantitated on a spectrofluorophotometer and the amount of polyamide **22** recovered from the cells determined by comparison to a standard curve of free polyamide **22**.

Figure 4. Determination of cellular localization of polyamide 22 using epifluorescence microscopy. SKBR3 cells were treated with either **22** at 0.5 μ M (***A/B***) or Bodipy alone at 5.0 μ M (***C/D***) for 4 hours. Cells were then washed 3X with PBS, fixed in acetone followed by rehydration in PBS. Coverslips were then mounted to a slide and visualized using an epifluorescence microscope. *Scale bar*, 50 μm.

Figure 5. Cellular uptake of polyamide 22 over time. SKBR3 cells were treated with 0.5 μM of polyamide **22** at the indicated times points and harvested. *Scale bar*, 50 μm.

Figure 6. Comparison of polyamides 2 and 22 in cellular uptake and binding studies. Competition between polyamides **2** and **22** for cellular uptake/transport utilized a 1 hour treatment of SKBR3 cells with: ***A***, **22** (0.5 μM), or ***B***, simultaneously with **22** and **2** at (0.5 μM and 5.0 μM, respectively). Chase studies for molecular binding site employed a 4-hour pre-treatment of SKBR3 cells with **22** (0.5 μM) followed by a 6-hour chase with: ***C***, water or ***D***, **2** (5.0 μM). *Scale bar*, 50 μm.

Figure 7. Comparison of cellular localization and binding pattern of polyamide 22 to other known DNA minor groove binding agents. SKBR3 cells were treated for 1 hour with: ***A/B***, polyamide **22** at 1.0 μM; ***C/D***, Hoechst 33342 at 2.0 μM; ***E/F***, Hoechst 33258 at 2.0 μM; ***G/H***, DAPI at 40 μM. *Scale bar*, 50 μm.

Figure 8. Localization of polyamide 22 in the cell nucleus using laser scanning confocal microscopy. SKBR3 cells were treated with 0.5 μM of polyamide **22** for: **A/B,** 10 hr;

C, 10 hr; and **D**, 28 hr. **B** is an enlargement of the boxed imaged in **A**. All images are 0.5 micron midplane sections.

Acknowledgements:

The epifluorescence microscopy was performed under the guidance and training of Dr. Nannette Stangle-Castor. The confocal microscopy was performed at the Confocal Microscopy and 3-D Imaging Facility of the School of Medicine and Biomedical Sciences at SUNY/Buffalo. Alan Siegel of the Microscopic Imaging Facility at SUNY/Buffalo provided valuable assistance with image processing and printing.

References:

1. Geierstanger, B. H., Mrksich, M., Dervan, P. B., and Wemmer, D. E. Design of a G.C-specific DNA minor groove-binding peptide, Science. *266:* 646-50, 1994.

2. Swalley, S. E., Baird, E. E., and Dervan, P. B. Recognition of a 5'-(A,T)GGG(A,T)$_2$-3' Sequence in the Minor Groove of DNA by an Eight-Ring Hairpin Polyamide., Journal of the American Chemical Society. *118:* 8198-8206, 1996.

3. Parks, M. E., Baird, E. E., and Dervan, P. B. Recognition of 5'-(A,T)GG(A,T)$_2$-3' Sequences in the Minor Groove of DNA by Hairpin Polyamides., Journal of the American Chemical Society. *118:* 6153-6159, 1996.

4. Swalley, S. E., Baird, E. E., and Dervan, P. B. Effects of gamma-turn and beta-tail amino acids on sequence-specific recognition of DNA by hairpin polyamides, J Am Chem Soc. *121:* 1113-1120, 1999.

5. White, S., Szewczyk, J. W., Turner, J. M., Baird, E. E., and Dervan, P. B. Recognition of the four Watson-Crick base pairs in the DNA minor groove by synthetic ligands [see comments], Nature. *391:* 468-71, 1998.

6. Trauger, J. W., Baird, E. E., and Dervan, P. B. Recognition of 16 Base Pairs in the Minor Groove of DNA by a Pyrrole-Imidazole Ployamide Dimer., Journal of the American Chemical Society. *120:* 3534-3535, 1998.

7. White, S., Turner, J. M., Szewczyk, J. W., Baird, E. E., and Dervan, P. B. Affinity and specificity of multiple hydroxypyrrole/pyrrole ring pairings for coded recognition of DNA, J Am Chem Soc. *121:* 260-261, 1999.

8. Dickinson, L. A., Trauger, J. W., Baird, E. E., Ghazal, P., Dervan, P. B., and Gottesfeld, J. M. Anti-repression of RNA polymerase II transcription by pyrrole-imidazole polyamides, Biochemistry. *38:* 10801-7, 1999.

9. Dickinson, L. A., Trauger, J. W., Baird, E. E., Dervan, P. B., Graves, B. J., and Gottesfeld, J. M. Inhibition of Ets-1 DNA binding and ternary complex formation between Ets-1, NF-kappaB, and DNA by a designed DNA-binding ligand, Journal of Biological Chemistry. *274:* 12765-73, 1999.

10. Gottesfeld, J. M., Neely, L., Trauger, J. W., Baird, E. E., and Dervan, P. B. Regulation of gene expression by small molecules, Nature. *387:* 202-5, 1997.

11. Dickinson, L. A., Gulizia, R. J., Trauger, J. W., Baird, E. E., Mosier, D. E., Gottesfeld, J. M., and Dervan, P. B. Inhibition of RNA polymerase II transcription in human cells by synthetic DNA-binding ligands [see comments], Proceedings of the National Academy of Sciences of the United States of America. *95:* 12890-5, 1998.

12. Harapanhalli, R. S., Howell, R. W., and Rao, D. V. Bis-benzimidazole dyes, Hoechst 33258 and Hoechst 33342: radioiodination, facile purification and subcellular distribution, Nuclear Medicine & Biology. *21:* 641-7, 1994.

13. Chang, C. H., Scott, G. K., Kuo, W. L., Xiong, X., Suzdaltseva, Y., Park, J. W., Sayre, P., Erny, K., Collins, C., Gray, J. W., and Benz, C. C. ESX: a structurally unique Ets overexpressed early during human breast tumorigenesis, Oncogene. *14:* 1617-22, 1997.

14. Chiang, S. Y., Burli, R., Benz, C. C., Gawron, L. S., Scott, G. K., Dervan, P. B., and Beerman, T. A. Targeting the Ets Binding Site of the HER2/neu Promoter with Pyrrole-Imidazole Polyamides, Journal of Biological Chemistry. *In Press, August:*, 2000.

15. Scott, G. K., Daniel, J. C., Xiong, X., Maki, R. A., Kabat, D., and Benz, C. C. Binding of an ETS-related protein within the DNase I hypersensitive site of the HER2/neu promoter in human breast cancer cells, Journal of Biological Chemistry. *269:* 19848-58, 1994.

16. Tripathy, D. and Benz, C. C. Activated oncogenes and tumor suppressor genes involved in human breast cancers. *In:* C. C. Benz and E. Liu (eds.), Oncogenes and Tumor Suppressor Gemes in Human Malignancies, pp. 15-60. Boston: Klurwer Academic Publishers, 1993.

17. Kapuscinski, J. DAPI: a DNA-specific fluorescent probe., Biotechnic & Histochemistry. *70:* 220-233, 1995.

18. Parks, M. E., Baird, E. E., and Dervan, P. B. Optimization of the Hairpin Polyamide Design for Recognition of the Minor Groove of DNA., Journal of the American Chemical Society. *118:* 6147-6152, 1996.

19. Arndt-Jovin, D. J. and Jovin, T. M. Analysis and sorting of living cells according to deoxyribonucleic acid content., The Journal of Histochemistry and Cytochemistry. *25:* 585-589, 1977.

20. Denison, L., Haigh, A., D'Cunha, G., and Martin, R. F. DNA ligands as radioprotectors: molecular studies with Hoechst 33342 and Hoechst 33258., International Journal of Radiation Biology. *61:* 69-81, 1992.

Figure 1

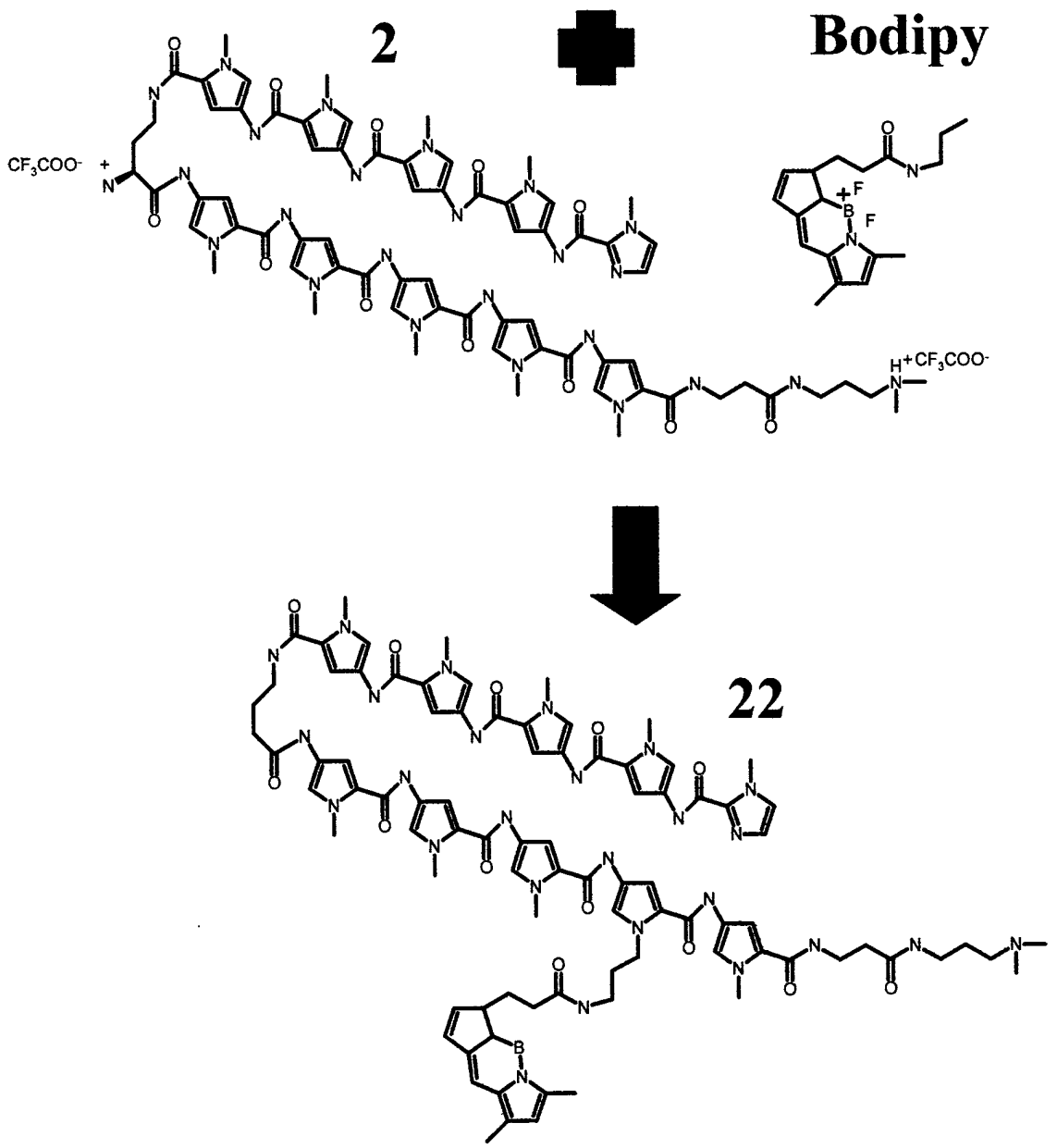

Figure 2B

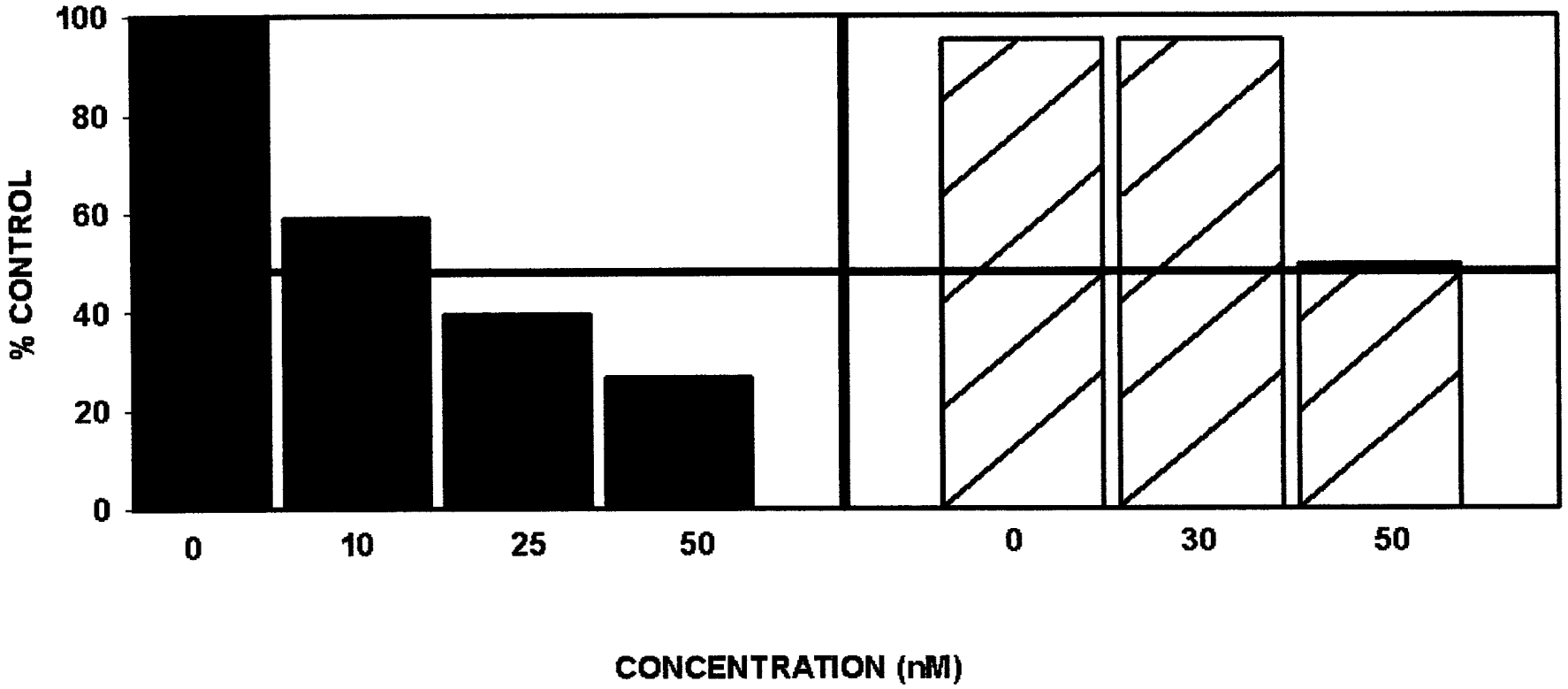

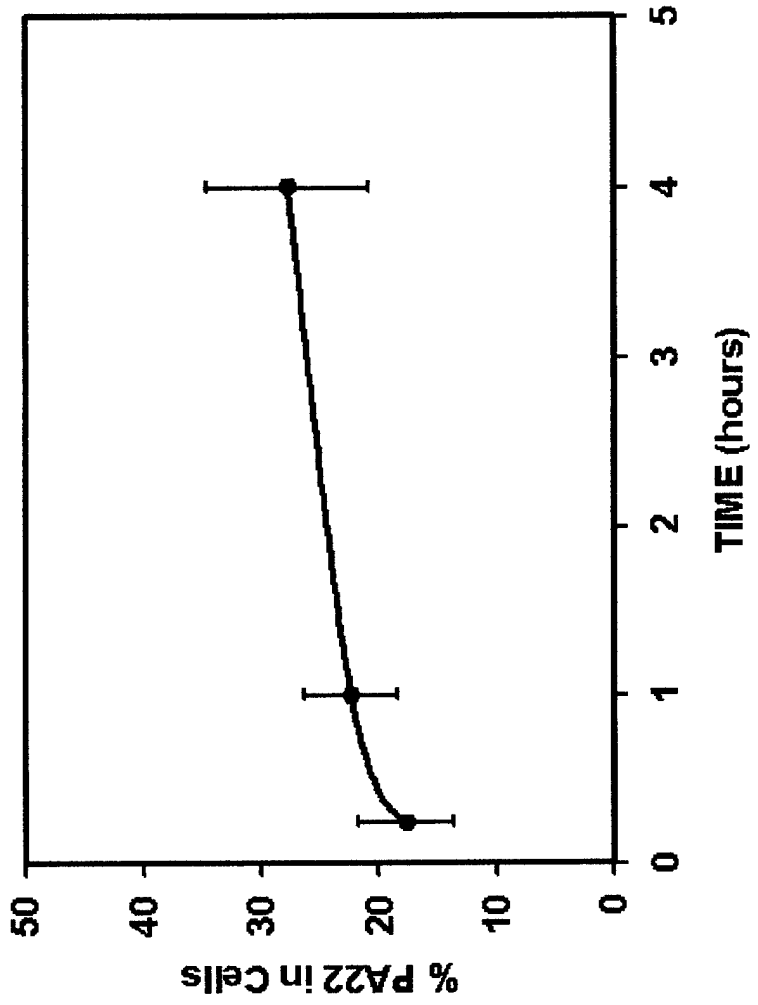

Figure 3

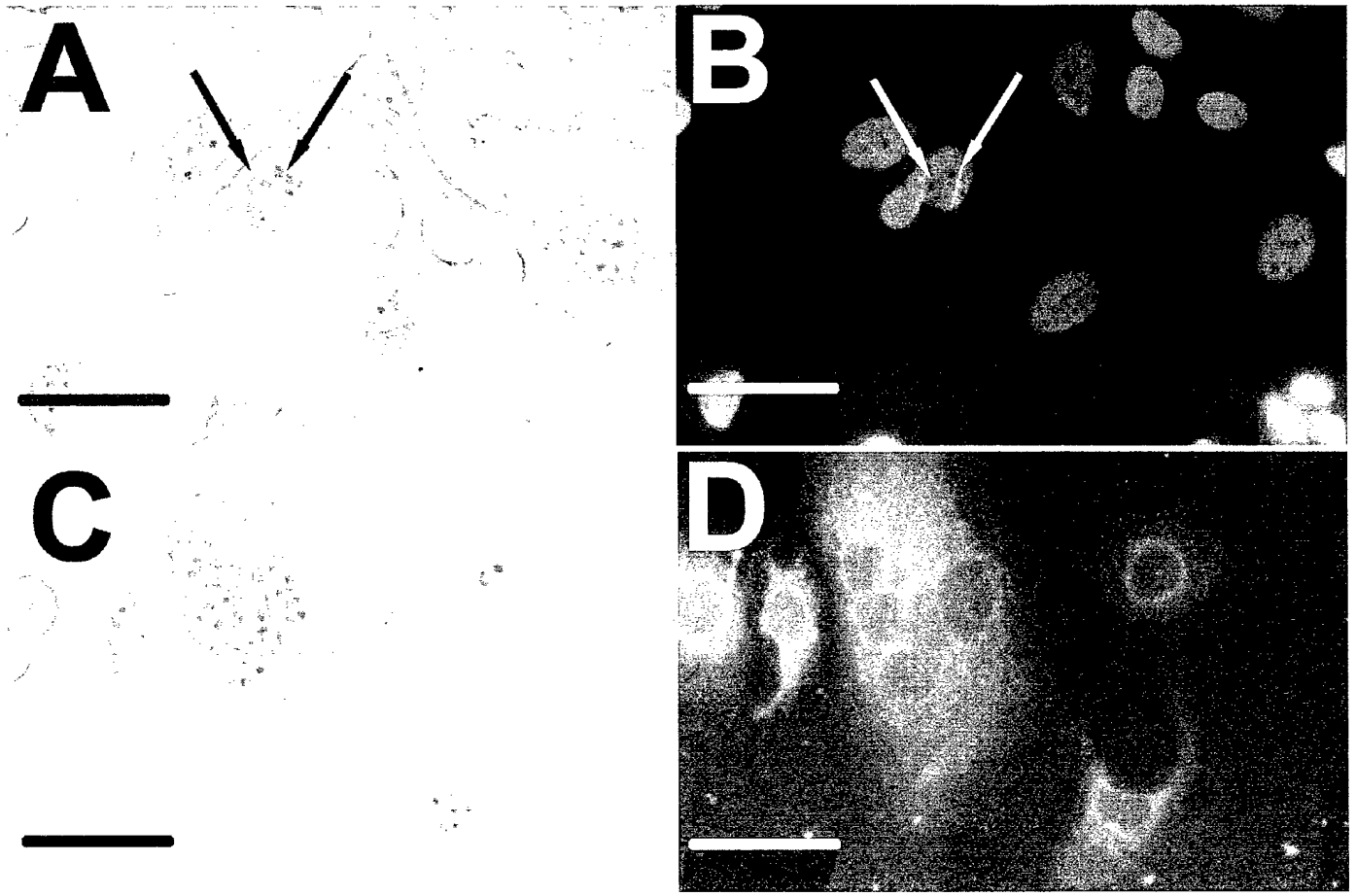
A
B
C
D

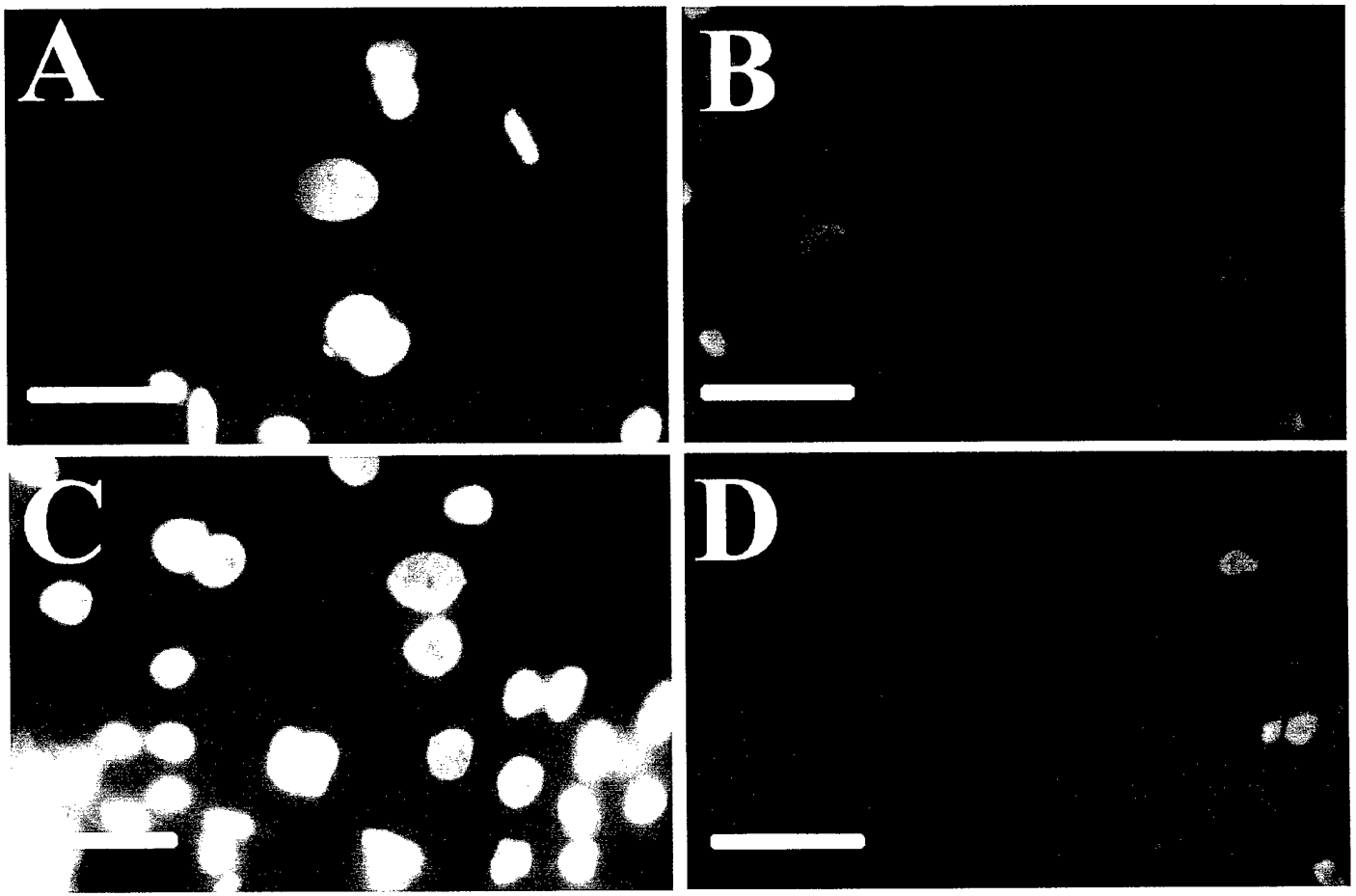
A
B
C
D

Figure 5

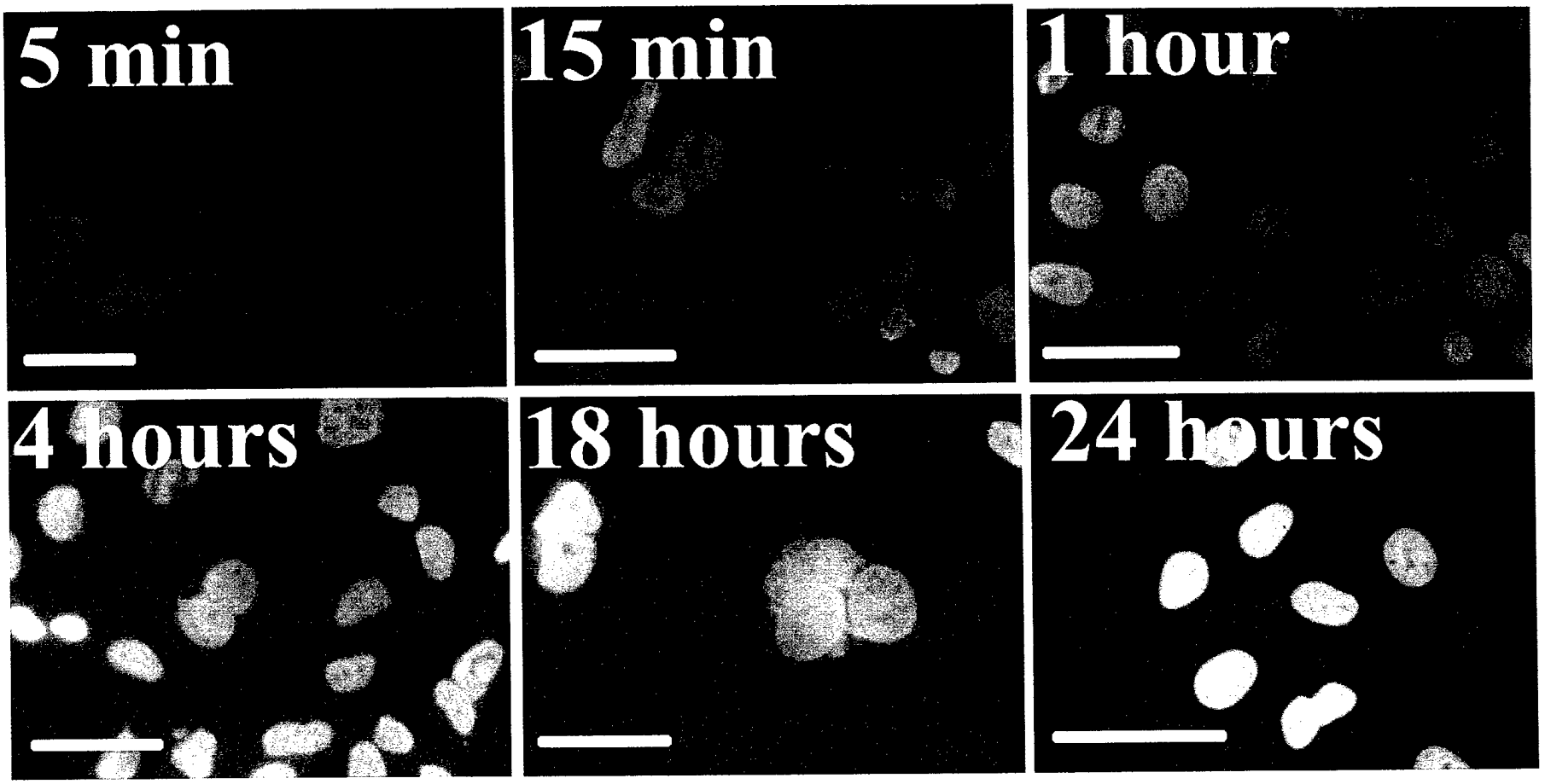

A C E G

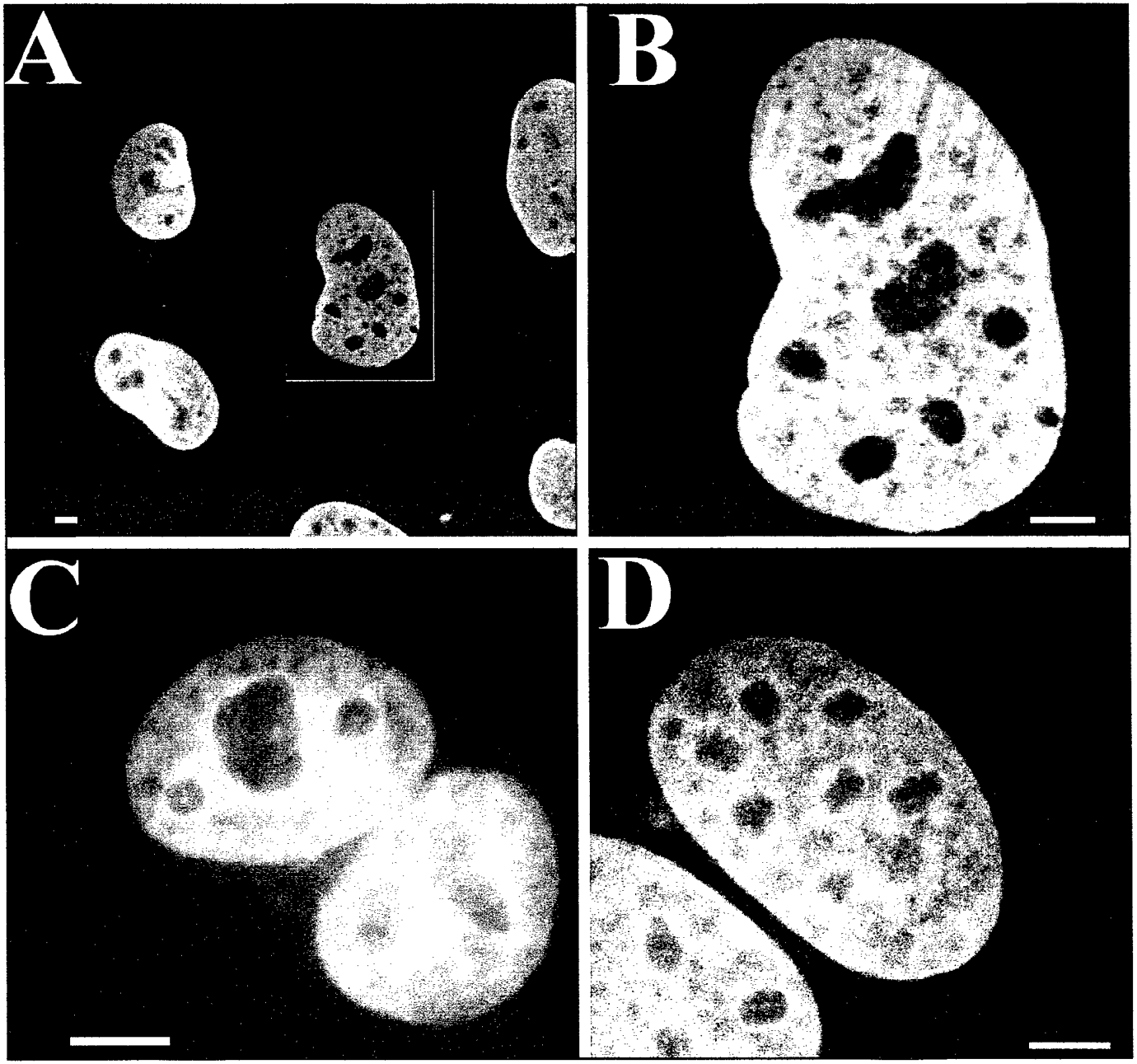
A
B
C
D